Application

APPLICATION OF CFD TO THE ANALYSIS AND DESIGN OF HIGH-SPEED INLETS

FINAL REPORT

25 MAY 1995

Prepared for:

NASA-AMES RESEARCH CENTER

MOFFETT FIELD, CA 94035

UNDER NASA GRANT

NCC 2-507

(NUMERICAL INVESTIGATIONS IN THREE-DIMENSIONAL INTERNAL FLOWS)

By:

WILLIAM C. ROSE

ENGINEERING RESEARCH AND DEVELOPMENT CENTER

UNIVERSITY OF NEVADA, RENO
RENO, NV 89557

TABLE OF CONTENTS

I. BACKGROUND

NASA has an ongoing interest in supersonic and hypersonic aircraft flowfield research. Their research efforts over the years have been intended to complement prospective air-breathing propulsion aerospace vehicles, such as the High-Speed Civilian Transport (HSCT) and the National Aerospace Plane (NASP), as well as other variants of these vehicles. Throughout the course of the present NASA Grant, the analysis of the flow within and the design of the inlet systems for such aircraft have been of particular interest. Computational Fluid Dynamics (CFD) is expected to play a large part in the analysis and design of such future aircraft because ground-based experimental facilities are limited and expensive to operate. The purpose of this Grant has been to apply, evaluate and validate various CFD tools for use in high-speed inlet design and analysis.

The present Grant has been supported by NASA's Ames Research Center and has spanned a period of several years. Work carried out and previously reported appears in References 1-12. This final report contains the status reports for CY 1994 and, in addition, is intended to summarize the findings over the lifetime of the Grant relative to the best use of CFD in high-speed, air-breathing propulsion inlet systems. In previous efforts under the Grant, both two-dimensional and three-dimensional CFD codes have been applied to inlet flowfield analysis and design. The Mach number range of the study has covered about 3 to 15. No new codes were developed in this effort, and only those available for use in an applied environment have been exploited. The codes applied here have included most of the currently-popular CFD codes at NASA-Ames.

Most of the efforts conducted under the Grant have examined the flowfield characteristics and performance of isolated inlet systems. In reality, of course, these inlet systems are installed on aircraft at various locations in various flowfields. The primary effect on the inlet of an installation on any aircraft is the modification of the oncoming flowfield and, particularly for surface-mounted inlets (as opposed to those mounted on pylons or other standoff devices), this modification is an increase in the oncoming boundary layer thickness relative to the cowl height of the inlet. Some efforts in the present study have been directed towards examining the effects of various oncoming boundary layer thicknesses and one major effort examined an inlet installed on a waverider hypersonic aircraft.

By way of background and for purposes of defining the terminology for the remainder of the report, the terms "analysis" and "design" are not used interchangeably here. The term "analysis" is used to connote the application of a computational fluid dynamics code applied on a grid appropriate to the contours of the hardware to produce a definition of the flowfield under a specific set of operating conditions, such as freestream Mach number, total pressure, etc. There is no necessarily-implied feedback from an analysis that will allow a modification of the contours or examine the potential effect that such a modification might have on a newly computed flowfield. On the other hand, the term "design" is strictly reserved to connote the development of hardware contours more-or-less specifically to meet a previously-set goal, subject to a set of constraints. "Design" implies a closed feedback loop for examining the flowfield results, deciding if they meet the design goal, and, if not, modifying the contours and recomputing the flowfield. This process

continues until the goal(s) are met. The definitions of these two terms should be kept in mind when they are used throughout the present report.

Although much discussion has been devoted to the promise of CFD as a useful design tool, little has been done to establish the current generation of high-fidelity CFD methods, such as full Navier-Stokes (FNS) solvers, as a realistic, credible component of a commercially-applicable design process for high-speed aircraft. Much more has been done in the use of low- and medium-fidelity methods, i.e., potential flow, Euler solvers and boundary layer codes, in the design process for external flows and, in fact, these codes are used routinely in aircraft design. In order to bring CFD codes to bear on the day-to-day design problems of supersonic and hypersonic inlets, significant effort beyond today's state of the art in applied CFD will be required. The present report discusses this type of effort.

In the past, high-fidelity CFD codes have been used almost exclusively as analysis tools without being applied to the development and/or derivation of the contours used in the definition of the high-speed inlet geometry. Several studies, some of those carried out by the present author, have used CFD as an analysis step in a "man-in-the-loop" inlet design process. This process is inherently iterative, done manually, and requires extensive efforts in order to even modify a previously-known design. One ultimate goal in terms of inlet design is to bring the use of state-of-the-art CFD inlet analysis codes to a level that will allow them to be used in an automated design code that frees the inlet designer from the above-mentioned tedium. In the

present study, an optimization code and a CFD code were used in order to demonstrate the path required to carry out an actual automated design process.

The notion of CFD code "validation," which is better described as a process of code evaluation, modification and, finally, validation is also discussed. Typically, this process is dependent on external sources of "truth," usually construed to be experimental data. The loop in the evaluation and code modification process may be highly repetitive before a truly validated code exists. Implied in code validation is code accuracy. However, even the term "code accuracy" is somewhat misleading since the overall accuracy of a code is dependent less on the numerical algorithms employed in the code and more on the grid upon which the code is applied. Another accuracy consideration is the appropriateness of the representations of fluid physics (e.g., turbulence model). Presumably, all modern CFD codes contain robust mathematics that are inherently accurate. With a sufficiently-fine mesh, the code would be accurate ("spatially accurate"), limited only by the fidelity of the turbulence model, and, if the user has a sufficient amount of computational time and patience, can obtain the ultimate, accurate solution. In reality, of course, trade offs between solution turnaround time, computer cost, the anxiety of the user and available resources have to be made, and accuracy typically suffers.

Independent of the absolute accuracy of a code, much can be understood about the sensitivity of the inlet geometry and other specific attributes of the hardware through a repetitive application of the code while varying parameters of interest. These so-called "parametric" studies are extremely powerful in learning about any flowfield, but are particularly important in

understanding the internal flowfields characteristic of high-speed engine inlets. The successful understanding of such flowfields through the parametric use of low- and medium-fidelity codes applied to engine inlets is spoken to by the great successes enjoyed in the 1960s and 1970s. Before the advent of useful CFD, design and understanding of high-speed inlet flowfields was achieved through the use of method-of-characteristics and boundary layer codes. Method-of-characteristics codes, of course, provide solutions to the inviscid, hyperbolic behavior of the full Navier-Stokes codes, while boundary layer codes provide solutions to the viscous, parabolic nature of the Navier-Stokes codes associated with flowfields near surfaces. In spite of the fact that neither of these code types is extremely accurate, the understanding of flowfields as a result of their repetitive application is undeniable. Greater understanding about internal flowfields from parametric analysis can be obtained from today's modern codes applied on, for example, a coarser mesh with its attendant inaccuracies but with the ability to produce a multitude of solutions for various parameters. **The idea that we lead to in this discussion is that it may be much more important to apply a given code to a flowfield of interest many, many times to understand the sensitivity of various parts of the flow to design parameters than it is to obtain one single, very-accurate solution from which little physical insight may be gleaned.**

The current, industry-wide goal is to bring computational fluid dynamics into the design loop for high-speed inlet flowfields. Although advancement in CFD methods applied to internal flows has tended to lag behind that for CFD methods useful for external flows, the current state of the art in supersonic and hypersonic inlet CFD allows for the analysis of mixed internal/external compression inlets with bleed, injection, normal shocks and subsonic diffuser flows (e.g.,

References 13-16). With this design goal, and the knowledge that the more simplistic, low- and medium-fidelity computational methods may be useful, we set out to use modern CFD to design inlets.

The current status of CFD codes is that they cannot "design" a high-speed inlet because they (and the meshes on which they are operated), although capable of simulating very complex geometries, lack a closed-loop interface that is required to modify the geometry after an analysis is made and, further, they lack the capability to judge the quality of a design at any point in the design iteration cycle. Currently, the design process of modifying an inlet geometry is done manually and typically requires much more time than the computation time for the CFD code. A human must analyze the CFD results and determine the modifications to the geometry that will improve the design. A human with many years of inlet design experience is currently required to effectively complete the process in most high-speed inlet designs. Ultimately, the goal of an automatic design capability is to remove this "man-in-the-loop" effort of analyzing the CFD results and then modifying the geometry and replace it with a pseudo-intelligent, computerized design program that would make modifications based purely on numerical correlations between calculated measures of quality and specific changes in the geometry to successfully design an inlet. Stay tuned.

During the course of the present Grant, both analysis and design efforts have been carried out. More analysis efforts were carried out because code evaluation, improvement and validation cycles were considered early in the study. As the study evolved, the design of a new Mach 10

inlet was undertaken using a man-in-the-loop approach. Later, the author was involved with an automated design procedure coupling a numerical optimization code used previously with external aerodynamic flows (NPSOL) (Reference 17) and an existing parabolized Navier-Stokes flow-analysis code (STUFF) (Reference 18). This coupling produced an automated program for the simple task of designing a two-dimensional, supersonic inlet/ramp combination with three independent ramp elements.

This final report outlines the historical approach to inlet design, including requirements for boundary layer mass removal (bleed) in order to control separation and to control the compression rate throughout an inlet. It looks at why some of these historical methods are important. It also examines the status of the currently-available CFD tools, including the turbulence models available, how robust the codes are, and the user-interface and the user-friendliness factors for various codes. The computation times per case (and, more importantly, the turnaround times) are discussed. This report summarizes many years of effort and does not necessarily cover all of the efforts conducted under the present Grant. It does present a fundamental approach to high-speed engine inlet design that will be required of any person, group of persons, code, group of codes or any combination of these to effect a successful inlet design.

II. HISTORICAL PERSPECTIVE

Once upon a time there was no CFD. However, jet aircraft and their inlet systems have been flying since the mid-1940s. In order to sustain successful engine operation, an inlet system must provide air at sufficient pressure, mass flow and flow quality (distortion) to the engine. The specific requirements vary throughout the flight regime for any given engine and vary substantially from engine to engine. For a relatively-low Mach number aircraft, say, for example, below Mach numbers of 1.3 to 1.4, a normal shock inlet is usually used. The total pressure loss across a normal shockwave is not substantially higher than across oblique shockwaves that might be created through multiple-ramp geometries at these Mach numbers. Beyond this Mach number, however, multiple oblique shockwave systems and distributed compression regions are used to produce the desired compression. This is true whether the inlet is nominally two-dimensional or axially symmetric. Early engine inlets were developed simply as a result of experimentation, even though the underlying mathematical descriptions of their supersonic flow had been known for nearly a half a century. Before analytical codes for solving the inviscid equations of motion relative to engine inlets existed, a graphical technique, known as the Hodograph, was used in conjunction with experiments to develop successful inlet contours. The Hodograph is simply a graphical solution for the wave-like behavior consistent with hyperbolic, supersonic, inviscid flow. These solutions, of course, were very tedious and yielded little information concerning the type of flow actually found in a complex inlet system.

The first really useful analytical technique for use in designing inlets was the method of characteristics, which is a solution of the inviscid flow equations. Much of the early evolution of

analytical tools for inlet design originated at NASA-Ames. Roy Presley first set down the relevant equations and boundary conditions for the method of characteristics applied to an engine inlet. These equations and boundary conditions were coded by Virginia Sorensen into a program later to become known as the "Sorensen Program" (Reference 19). A version of that code (known as MOC 76) is still in existence today (having its thirtieth birthday) and is operable on various NASA-Ames machines. This code and other method-of-characteristics programs solve for the wave-like structure of supersonic flow using waves of both families (that is, waves from right-running and left-running characteristics, the behavior of which is critical to the determination of successful inviscid inlet contours). The Sorensen program was used successfully to analyze various proposed inlet contours for the USA SST program in the mid- to late-1960s. The code originally required up to a five-day turnaround when run on an IBM 7094, including plotting of the "characteristic net" or "Mach net," to obtain a two-dimensional solution. Today, this code would take approximately five seconds on a workstation to solve the same flowfield.

The importance of method-of-characteristics programs is that they recognize the wave-like nature of the inlet compression process and, furthermore, that the constructed Mach nets are intuitive in that they show the designer which portion of the inlet geometry affects what portions of the flowfield. Although it may sound like a trivial statement, the distinguishing feature of internal aerodynamics is that there are bounding surfaces that capture and reflect and re-reflect compressions throughout the inlet. This is clearly distinct from the external aerodynamics situation, where, usually, a single surface is involved with the outer boundary of the flow equal to the ambient conditions, or wind tunnel freestream, as the case may be. Method-of-characteristics

program results are very useful to the internal flow designer in finding where either overcompression or undercompression from the wave reflections and re-reflections is occurring throughout the inlet system. When the compression process is not significantly influenced by viscous effects, i.e., from boundary layers, shear layers or separation regions, the portrayal of the flow with these simple codes is quite good. In fact, during the early analytical efforts using this type of code, particularly those relating to the design of the SR71 axially-symmetric inlet and the designs for the USA SST inlets during the late 1960s, these codes were quite adequate. This is true because at lower flight Mach numbers, say, between 1.4 and 2.0, viscous effects are virtually insignificant except as they affect the stability of a terminal normal shockwave. In order to stabilize this shockwave within the duct, boundary layer mass removal, hereinafter known as "boundary layer bleed," must be employed. Later, boundary layer bleed was shown to be required at the location of oblique shockwave boundary layer interactions for higher Mach number inlets. Those under study in the late 1960s were designed, typically, for Mach numbers between 2.0 and 3.0. Experimentally, boundary layer mass removal rates were approximately 3 to 5% of the total inlet capture mass flow. This is a relatively small percentage of the total flow, although it represents nearly 100% of the viscous flow. Once the viscous flow was removed, inlets were found (not surprisingly) to behave in a manner nearly identical to that predicted through the method-of-characteristics codes. The percentage of boundary layer bleed required increases as the Mach number increases. If the empirical bleed curves developed for SST-type designs were extrapolated to a Mach 5 inlet, estimates of boundary layer bleed requirements would skyrocket to 30 to 40% of capture mass flow, clearly an unacceptable amount of boundary layer bleed. The reasons for this are discussed next.

It was realized during the 1970s that boundary layer bleed was experimentally invoked in the inlet designs of the late 1960s simply to remove the effects of viscosity, rather than specifically to control boundary layer separations. This, again, is consistent with the notion that when few or no viscous effects are present, inviscid methods do a good job of capturing the flowfield, a self-fulfilling prophecy. When viscous effects become more dominant, that is at Mach numbers much above 3, stand-alone boundary layer codes can be used to estimate them. One such inlet boundary layer code (IBL) (Reference 20) was developed at NASA-Ames specifically to examine boundary layers occurring in flowfields typical of those in a high-speed inlet. Ad hoc procedures for coupling (i.e., remerging the viscous and inviscid portions of the Navier-Stokes equations) method-of-characteristics and boundary layer codes in so-called multi-layer analysis methods were also prevalent during the 1970s. These multi-layer methods (e.g., References 21, 22 and 23) attempted to describe both the attached boundary layer flow and those boundary layers subject to the strong adverse pressure gradients resulting from shockwave/boundary layer interactions occurring within the internal flowpath of the supersonic inlet. These coupled analyses were cumbersome, typically difficult to use, and certainly were not design tools.

Because of the limited computer resources available during the late 1960s and 1970s, virtually all flowfields were calculated as though they were two-dimensional. One three-dimensional method-of-characteristics program was developed at NASA-Ames by John Raikich. However, the code was also very cumbersome, not user-friendly, and remained virtually unused for inlet flow analysis.

Attempts to design (without consideration of viscous flow effects) a Mach 5, axially-symmetric inlet were carried out in the early 1970s. This inlet model was fabricated and tested in the NASA-Ames 3.5-ft Hypersonic Wind Tunnel. The test was largely unsuccessful in that the design contraction ratio for this inlet could never be obtained experimentally for reasons that we now know are associated with the unaccounted-for, very thick boundary layers present at this high Mach number.

In one of CFD's earliest forays into developing a code specifically for inlet analysis, the shock-capturing algorithms exploited by computational personnel at NASA-Ames were incorporated into an inlet analysis program by Presley and Kutler (Reference 24). This code solved the inviscid flow equations in three dimensions and gave a good account of the flowfield within representative supersonic ($M \approx 2.5$ to 3.0) inlets. Shockwaves of arbitrary strength could be captured with this code, as opposed to the ultimate breakdown of a method-of-characteristics code when distributed compression fields become strong enough to form shockwaves.

The dawn of real CFD was ushered in by MacCormack (Reference 25). An application (inspired by supersonic flow in an inlet) of his viscous cratering code was the solution of a laminar boundary layer/oblique shockwave interaction (Reference 26). MacCormack's algorithm was picked up and used by several others. Most notably for inlet analysis, Ajay Kumar from NASA-Langley applied the MacCormack algorithm with supersonic inlet-type boundary conditions to produce NASCRIN, a functioning, two-dimensional analysis code (Reference 27) that was used

extensively throughout the 1980s. This code and its three-dimensional version, SCRAM 3D (Reference 28), were used in the present investigation.

Subsequent to the Kumar inlet code, codes developed by Molvik (TUFF and STUFF in Reference 18), Lawrence (UPS3D in Reference 29) and Buning (OVERFLOW in Reference 30) have been employed in analysis and design during the course of the present study. The way in which a code is used to analyze the flow within a set of inlet contours and how it can be used in design is the subject of the rest of this report. The following section presents an example of a design process carried out in the early 1980s using the historical approach and pre-CFD methods. Modern CFD analysis codes applied to a newly-designed inlet and the redesign of another are then discussed.

III. EXAMPLE OF AN "INLET DESIGN"

This section of the report describes the process used to design the surface contours for what is commonly known as the "NASA Mach 5 inlet" (Reference 31). The author was one of the designers of these aerodynamic contours and this design process serves as an excellent example to show the path which must be taken to actually design a supersonic inlet system. This example is relevant as it is the only unclassified, functioning (contains boundary layer bleed), variable-geometry inlet system designed to be operated above Mach 3 that has been built and successfully tested. The inlet served as the focus of an initial stand-alone research program and was later integrated into and tested extensively in the National Aerospace Plane (NASP) program.

Contour development for an inlet capable of providing flow to a ramjet engine throughout the Mach number range from 3 to 5 was carried out as part of an Air Force requirement for a Mach 5 penetrator aircraft. The Mach 5 inlet has a variable-geometry design in order to meet the design goals while minimizing aircraft weight and boundary layer bleed amounts. Most inlet designers concede that variable geometry will be required to produce acceptable flow to ramjet or scramjet engines and this geometry will be scheduled according to the operating Mach number range. The design criterion for the Mach 5 inlet was to deliver a stable air supply to the ramjet engine over an operating Mach number range from light off (at approximately 0.9) to the cruise Mach number of 5.0. Although the inlet requirements for operation at the lower portion of this Mach number range were kept in mind, the detailed design effort was limited to the Mach 3 to 5 range, where the ramjet would constitute the sole source of propulsion. Boundary layer bleed is

employed extensively throughout the two-dimensional contours to minimize the potential adverse effects of boundary layer separation.

The compression process for the Mach 5 inlet model consists of three ramps with three discrete shockwaves followed by an internal flow with distributed compressions developed by the cowl and centerbody contours downstream of the cowl lip, a throat section with a terminal shockwave, and a conservative subsonic diffuser. The three-ramp system was chosen in order to reduce the overall inlet size and increase the total pressure recovery ahead of the cowl. The first two ramps maintain a constant deflection angle of 5 degrees each relative to the reference waterline. The third ramp is a variable-angle ramp, set for a 5-degree additional deflection at the on-design Mach number of 5 and reduced with Mach number, according to a schedule, to a very small deflection for a Mach number of 3. The remainder of the centerbody of the inlet is articulated in accordance with this Mach number schedule. The cowl remains fixed for all flow conditions. The fundamental nature of the initial two-dimensional ramp compression is carried through in most modern two-dimensional inlet systems. Downstream of the cowl lip, a supersonic compression section exists in which the method-of-characteristics program was used in the design to obtain contours that produced a relatively-short, lightweight inlet. The basis of this short, lightweight design for the internal flow portion was the use of a combination of the cowl shockwave compression, followed by a wave cancellation section on the centerbody, with the remainder of the internal compression coming from nearly isentropic, non-focused compression regions. The final contours for the inlet at the design Mach number of 5 are shown in Figure 1, along with the method-of-characteristics "Mach net" for the solution. This type of compression

process is different than those used previously for other supersonic inlets in which reflective, discreet, oblique shockwaves ahead of the terminal shockwave section were used to produce most of the compression. The reason for using the non-focused, continuous compression concept to produce most of the compression here was to avoid sudden, strong, adverse pressure gradients (at the higher Mach numbers) that would separate the boundary layer flow.

The Mach 5 inlet design was carried out using a method-of-characteristics program (Reference 32) and a boundary layer code (Reference 20) run iteratively to analyze hypothetical contours. This externally-coupled viscous/inviscid calculation scheme was used because of the state of the art of CFD at the time of the Mach 5 inlet design. Parametric variations which involved various locations of boundary layer bleed, bleed rates, and inlet contour changes were simply not amenable to CFD then. Two-dimensional pressure distributions from the method-of-characteristics code were imposed on the boundary layer code and a displacement thickness was calculated up to the point of boundary layer separation (usually occurring at the first shockwave/ boundary layer interaction). Bleed was then introduced into the boundary layer program. Amounts of bleed sufficient to eliminate boundary layer separation and allow the boundary layer code to continue were determined. This iterative process was carried throughout the inlet on the ramp (centerbody) and cowl surfaces. The result was a pair of displacement surfaces to modify the aerodynamic surfaces used in the method-of-characteristics program and a schedule of boundary layer bleed to be applied as a function of Mach number and location on each of the surfaces. The inlet was originally designed using only two-dimensional methods with the understanding that some three-dimensional effects would be present. (Many subsequent efforts

using various CFD codes have analyzed the flow within this three-dimensional inlet model (References 13 through 16, for example).) This is the quintessential "man-in-the-loop" design process.

As noted previously, if one were simply to extrapolate boundary layer bleed requirements from lower Mach number inlet testing, an unacceptably high amount of boundary layer mass flow would have to be removed. The philosophy adopted here was to remove only enough boundary layer flow to eliminate boundary layer separation. With this design philosophy, the viscous displacement effects of the remaining boundary layer flow became integrally linked with the compression process and, hence, the design of the contours, and, as a result, the Mach 5 inlet removed much less boundary layer mass than was previously estimated to be possible. Because of the relatively-high Mach number considered in the Mach 5 inlet design, the boundary layers are very thick and can significantly alter the compression process throughout the inlet from that predicted with an inviscid flow code. The effects of the boundary layers in the Mach 5 design were estimated through an iterative process in which the boundary layer displacement thickness distribution through the inlet subject to the pressure distribution derived from inviscid flow analyses was calculated. The displacement thickness distribution was then used to define new contours for subsequent inviscid analysis of the flow. This iterative process was repeated many, many times. For example, during the course of the Mach 5 inlet design, the IBL code was run for over 1,000 cases. Each of these cases varied the pressure and bleed rate distribution. Over 100 inviscid analyses were carried out to select between a "long," "short," and "medium" inlet and to optimize the selected inlet (A3M, the medium length inlet).

An important aspect of inlet design can be discussed with the aid of Figure 1. This figure shows the Mach number and pressure distributions on the ramp and cowl surfaces for the internal flow portion of the Mach 5 inlet. These contours are the final ones for the design Mach number of 5. The Mach net shown in the center of the figure starts with the cowl shockwave caused by a 10-degree turn of the ramp flowfield that impacts the center body at a "shock-cancellation" location. Although later in the NASP program the notion of shock cancellation was largely invalidated for very-high Mach numbers, its use in the Mach number range between 3 and 5 appeared to be credible. The remainder of the Mach net shows the all-important internal flow interactions dominant in efficient high-speed inlet systems. The pairing of non-canceling centerbody and non-canceling cowl surfaces to achieve a somewhat-uniform pressure rise is evident. Figure 1 represents the culmination of approximately two years of effort by numerous people to achieve what was thought to be the shortest inlet design that produced a relatively uniform flowfield at the entrance to the terminal shockwave section. The expected pressure recovery at the ramjet (including the terminal shock) was estimated to be approximately 50%. Although this sounds very low by SST and HSCT goals, it was found to be a good target pressure recovery value (and was experimentally verified) for the design Mach number of 5.

The non-intuitive contours for the internal compression portion of the inlet shown in Figure 1 resulted from the personal experience of several inlet designers, notably Ed Perkins. The number of trial calculations used in this design would be virtually prohibitive to do with CFD in three dimensions even with today's state-of-the-art computational methods and hardware. The logical extension of the man-in-the-loop iterative design process used in the Mach 5 inlet design

today would amount to running a code, such as the OVERFLOW code (Reference 30), in two dimensions (three planes) until the desired contours were developed, then performing limited, three-dimensional calculations to assess the compressive effects of the sidewall flowfields.

The revealing nature of the Mach net, typical of that shown in Figure 1, is vital to the design of a high-speed inlet system, yet, modern CFD graphics virtually never represent the flowfield in this manner. As such, the users of these codes have been remiss in obtaining the maximum potential in use of the computed results. The PLOT3D and FAST post-processing codes do not allow direct portrayal of a Mach wave-oriented field that would be very useful in an inlet design or redesign (although the FAST code allows gradient-based functions to show some of this type of behavior). This seems to be a case where the old solution displays were better than the new in that the link to the designer and his/her modifications were much more lucid.

IV. DISCUSSION OF CODES USED IN THE PRESENT STUDY

IV.1 Code Requirements

In general, a code must possess four fundamental attributes to be useful in an inlet design cycle:

1. Applicability
2. Accuracy
3. Short Turnaround Time
4. Ease of Use

In addition, grid generation must be rapid and extremely user friendly to be useful in a design. (Wong's first law: "As supercomputers reach the speed of light, grid generation processes slow tremendously.")

The applicability of a CFD code to the analysis and design of internal flows and, specifically, high-speed engine inlets, is embodied in two parameters. The first is the type of boundary conditions (i.e., compatibility with mixed compression internal flows) that are invoked throughout the normal use of the code. The second is the code's user interface to define the characteristics of the engine inlet, such as the position of the cowl surface, the beginning of the ramp, the exit flow conditions, and the location and amounts of boundary layer bleed.

The importance of the user interface aspect of code applicability cannot be understated. As an example, in the early phases of the current Grant, in concert with the beginning of the NASP program, the CFL3D code from Langley was obtained and attempts were made to run the

code in an inlet environment. The code was written primarily for use as an external aerodynamics analysis code and, as best could be detected, had rarely been used to analyze internal flows. The lack of familiarity with the code, the unavailability of "nearby" code support, and the poor user interface were sufficient to eliminate that code from further consideration in the remainder of the present study.

In contrast to the CFL3D experience, the originally-coded Kumar code (SCRAM3D) from Langley was specifically coded and used for engine inlet analyses. Thus, the input parameters were consistent with those expected by an inlet designer. For example, input flow conditions of Mach number, total pressure and oncoming flow angularity were directly-user-supplied inputs. The location of the cowl and ramp leading edges and other inlet-specific parameters were identified with highly mnemonic code variables and were easy to follow, both in the input process and in the coding itself. Thus, when it came time to extend the capabilities of the original Kumar code, it was relatively easy to do. The extension, carried out at NASA-Ames, was to allow the code to be used with a multi-block grid rather than the original single-block grid to calculate the flow both within and external to the inlet.

No accuracy problem exists other than the prescription of an accurate turbulence model. Now, we return you to reality. A numerical algorithm can be considered to derive its accuracy based on the order of the polynomial that can be embedded within the discretization of the flowfield. In general, since the mid-1970s, no seriously-proposed algorithm has been found to be mathematically inaccurate. Mathematical accuracy, here, is defined as the ability to produce "the"

answer to the differential equations of fluid motion given a sufficiently-fine grid. In reality, the accuracy is uniquely tied to not only the turbulence model, but also to the size of the grid. In turn, the size of the grid is tied to the topic discussed next, code turnaround time. Thus, as might be perceived, the issues of accuracy and turnaround time boil down to a trade off. Obviously, the more refined the mesh, the more nodes are contained in the mesh (about a million nodes are required for a three-dimensional inlet to resolve the relevant fluid mechanics) and the more operations per time step/code step will be required.

Accuracy and resolution of turbulent boundary layer flows for inlets is keyed to what is really important in the compression process. For internal flows, the primary characteristic of the viscous flow to be accurately modeled in CFD is the displacement effect of the various layers encountered. Resolution of the local skin friction, for example, is not necessarily required in order to obtain a very useful engineering estimate of the displacement thickness. Even a cursory resolution of the boundary layer displacement thickness in a CFD code is sufficient to quantify the effects that the viscous layers might have as perturbations to the compression process. Thus, in order to use the code parametrically, it may be useful to forego detailed accuracy (including resolution of the near-wall properties) initially to minimize turnaround time and then return to a more refined grid at some point later in the study when the parametric issues have been resolved. More refined meshes allowing near-wall properties to be resolved might be required when separation or inlet operability (unstart) calculations are of interest.

The use of various turbulence models (all other parameters held constant) in a given code represents another trade off. Some turbulence models are known to be highly inaccurate in certain situations, while no turbulence model is known to be accurate in all situations (as demonstrated in the NASP program). For example, a common situation in inlet flowfields is the propensity of the commonly-used Baldwin-Lomax turbulence model (or realizations of that model in a code) to tend to predict boundary layer separation too early and, when boundary layer separation is predicted, it is typically too extensive. On the other hand, substantial reductions in code turnaround time can be achieved using this model. Two- or other-multiple-equation turbulence models tend to increase turnaround time and there is no known reason to believe that the answers derived therefrom are significantly more accurate.

The notions embodied in this discussion are clearly reminiscent of those described in the introduction of the present report in that the ultimate use of a code may not hinge at all on the determination of one extremely-accurate, as-best-as-all-can-possibly-be solution, but rather, on the ability of a code to be used many, many times to analyze various inlet contours, to have those contours changed and the codes rerun until a better understanding of the flowfield is obtained and the design objectives are satisfied.

Turnaround time is dependent upon the power of the computational hardware, the effort required to initiate a solution (including the grid generation phase), the actual wall clock time per solution and the post processing/analysis time. An applications engineer is not willing to wait long to get an answer; as is crudely put, "I'd like to have the answer before I forget the question."

Historically, codes which now seem trivial to use (for example, method-of-characteristics or boundary layer codes) had turnaround times when they were used of between one and five days. Thirty years later, CFD codes have turnaround times between one and five days. Of course we get much more information in that amount of time from the modern codes. It appears that we are willing to wait "less than one week" to get results. In a "man-in-the-loop" design process, it may be unrealistic to believe that a CFD solution can be obtained, post processed, studied, and understood and that intelligent modifications can be made to the design in significantly less time than that.

A revolution in turnaround time came with the changeover from the predominantly-used, time-accurate algorithms, such as, for example, the time-split MacCormack method embodied in SCRAM3D, to more modern algorithms, embodied in the present version of TUFF or OVERFLOW. Turnaround time can also be strongly influenced by the desire (or requirement) to have a time-accurate calculation rather than simply looking for a time-independent solution that may evolve after only a very small number of steps of the code, none of which is time accurate. . In general, time-accurate solutions are not required in a routine inlet design cycle, but can be used in limited, special cases, for example, when one seeks to understand the effect of an inlet unstart or a gust.

CFD codes and their application with respect to engine inlet design do not exist independent of the grid on which the equations of motion are solved. The effects of the grid can be first order in terms of the accuracy and usefulness of the solution. Aside from the grid density

issues discussed previously, the clustering of grid points is of concern. Clustering techniques, through various automated gradient allocation schemes ("adaptive gridding"), have been used successfully for various classes of problems. One class of problem that one might think is highly amenable to adaptive gridding is the solution of flow within high-speed engine inlets. "Cartoon"-type inlet flowfields, such as those represented by the early NASP inlet lines, are, in fact, very amenable to the application of adaptive grid technology. This is true since the primary fluid mechanics features of the cartoon-type inlet flowfield are the viscous boundary layer (and its required nearwall clustering) and simple shockwaves. The grid, of course, can be clustered manually along the expected locations of the shockwaves, as shown in Figure 2 for the forward portion of the grid used in modern solutions of the flow within the Mach 5 inlet. Use of automated adaptive grid schemes will easily identify the strong gradient properties of these shockwaves and cluster the grid accordingly, producing somewhat the same density as that shown.

In reality, for practical inlets with both distributed and discreet shockwave compression present within the same inlet flowfield, adaptive grid clustering appears to be less useful since regions of strong-gradient and weak-gradient compression are generally of equal interest. The relaxation of grid-spacing characteristics to allow clustering in strong-gradient regions reduces the accuracy of the code in other portions of the flow when a fixed number of grid points is used within a computational domain. For time-dependent flowfields, recent successful efforts have demonstrated the usefulness of time-dependent adaptive gridding. However, in the present study,

with a few notable exceptions, almost all of the effort has been focused toward obtaining time-independent solutions, and adaptive gridding techniques have not been invoked.

In the present study, the grids were generated either by a locally-written code for inlet flowfields called GRID3D or, most recently, through various versions of the GRIDGEN program (Reference 33) and a practical, inlet-oriented version referred to as QUICKGEN (Reference 34). Grids used throughout this study typically employ only nearwall clustering with the expectation that boundary layer separation effects are minimized and, thus, the important viscous forces are contained within the nearwall cluster grid. Within the internal flow portions of the inlet, rectangular, two-dimensional and three-dimensional grids have been used extensively. Pressure rises through shockwaves are smeared (amounts dependent on the algorithm) on these grids and the pressure rises might be slightly different than those that could have been achieved through an optimized grid, but the requirement for repetitive application of the grid generator dictates simplicity. On the other hand, the flowfield resolutions in the distributed compression process are not lost in these simple grids. Clearly, an ideal situation is increased computer power that allows much finer grid resolution to be used to obtain a solution within the desired turnaround time. Efforts in the present study were limited to grid definition consistent with the minimization of turnaround time and the maximization of parametric variations in order to design and/or redesign various internal flow contours.

IV.2 Comments on Specific Codes Used in the Present Study

IV.2.1 The SCRAM3D Code

The SCRAM3D code is based on CFD's finest hour: the advent of the MacCormack time-split, explicit, second-order-accurate algorithm for computing fluid flow. The boundary conditions applied to the code are user-friendly and are specific to inlet flowfields. The only drawback to the Kumar codes (Reference 27 for the 2D code, NASCRIN (which is referred to here as SCRAM2D) and Reference 28 for the 3D code) is that they are based on the explicit algorithm which requires an inordinate time per solution, involving upwards of thousands of time steps to achieve a time-independent solution. The MacCormack algorithm is largely bullet-proof, is known to be accurate, and is known to be capable of resolving relevant aspects of inlet flowfields, as shown by the present author in the dark ages of CFD (References 35 and 36). The three-dimensional code was modified in the course of the present study to accommodate multi-grid solutions. This code is still one of the cornerstones in the arsenal of CFD inlet analysis codes. It is extremely user-friendly and can be applied to virtually any internal flowfield describable on a nominally orthogonal mesh. The two-dimensional version can be run on a work station with a five to ten minute turnaround time. In the course of the present study (References 1-8), many numerical representations of turbulence were explored, ranging from the simple Baldwin-Lomax model originally coded by Kumar to Cebeci-Smith-type models with ad hoc "lag constants" to account for the known, non-equilibrium behavior of boundary layers subject to strong adverse pressure gradients. The three-dimensional version running on a 0.75 to 1.25 million node mesh requires about 100 hours of Cray C-90 time with about a two-week total turnaround time. This latter point limits its usefulness in a design cycle.

IV.2.2 The UPS Code

The UPS (UPS3D) code is a parabolized Navier-Stokes (PNS) code (Reference 29) developed at NASA-Ames by Scott Lawrence that has been used in the present study to define the boundary layer and initial shockwave characteristics for sharp leading edge inlet flowfields. Why use a code such as this in today's world of full-blown CFD? Simple -- accuracy and reduced overall turnaround time. No full-blown CFD code can be run on a grid that maintains the fine-mesh accuracy deliverable with the UPS code. Since the code is spatially-marched, a minimal number of streamwise planes are resident in memory at any time, so that this code may actually be operated in a work station environment. Going back to the original notion of inlet design, for a very-high-speed inlet, the flowfield at the nose of a sharp leading edge inlet sets the stage for the remainder of the flowfield. This hypersonic, viscously-interacting flowfield has never been accurately resolved with FNS codes applied on any sort of reasonable grid. Thus, results from the UPS code are valuable for rapidly examining boundary layer growth and the attendant, external "inviscid" flowfield. The UPS code was used here to solve the forebody flowfield and then to provide inflow conditions to the rest of the inlet flow describable with FNS codes (Reference 9). The algorithm is modestly robust. The bad news? The UPS code is written and structured primarily as a research code and not as an applications code designed to present a user-friendly, man-code interface. The inputs to the UPS code are Mach number and Reynolds number. Reynolds number, although obtainable from Mach number, pressure and altitude considerations, is not the parameter that rolls off the tip of an inlet designer's tongue. A pre-processing program was developed in the present study to input the inlet-type parameters and produce inputs to the UPS code. (The same situation exists for the STUFF/TUFF and OVERFLOW codes.) The UPS

code basically generates its own grid with a spatial evolution, so that even though the user interface is not inlet tolerant, the total amount of effort required to obtain a solution for a given inlet is typically not large. This modern "boundary layer" code is another staple in the inlet designers repertoire. An example of the effective use of the UPS code when coupled with a FNS code for inlet analysis is shown in Figure 3.

IV.2.3 The STUFF and TUFF Codes

The STUFF and TUFF codes (Reference 18), written at NASA-Ames by Greg Molvik, involve the use of modern, finite-volume, upwind, TVD algorithms and are very useful in inlet design. The user interface has been developed in the present study to provide inputs for Mach number and total pressure. The TUFF code is a time-marched discretization of the equations of fluid motion. This code has been primarily applied by its developer to combinations of internal flow and combustion with a full, attendant set of hydrocarbon combustion constituents. In the present study, the TUFF code was used in an attempt to describe the fully-interacting (with possible boundary layer separations) flowfield within the Mach 5 inlet. Comparisons between the results of this code and the Kumar code were quite good even though the TUFF code could not be successfully operated by the present author with an external flowfield (multi-block). The STUFF code is a spatially-marched subclass of the TUFF coding. It, along with the UPS code, can provide excellent first-cut analyses for boundary layer growth and forebody compression processes. An example of the comparison of the results from the STUFF and UPS codes is shown in Figure 4 along with experimental boundary layer and shockwave data from the Mach 5 inlet (Reference 14). A combined analysis using the STUFF code and SCRAM2D for the elliptic

portion of an inlet flowfield is shown in Figure 5. Cray C-90 turnaround times for these codes when generated with reasonable (about a million nodes in the 3D case), inlet-type grids are approximately half a day and 4 days for the 2D and 3D versions, respectively.

IV.2.4 The OVERFLOW Code

The OVERFLOW code, written by Peter Buning (Reference 30), is the current crown jewel in the NASA-Ames repertoire of full Navier-Stokes CFD codes. The code is written with a very general set of boundary conditions reminiscent of the class of boundary conditions used in CFL3D. However, in contrast to CFL3D, the OVERFLOW code can be easily used by applications engineers. Either the ARC3D or F3D algorithm can be selected. In this study, the ARC3D option was used for speed and robustness. A useful selection of turbulence models is available. However, in the present study (in the interest of achieving minimum turnaround times, as opposed to lengthy, one-of-a-kind calculations), the Baldwin-Lomax model was used mostly. The OVERFLOW code was modified in the course of the present study to allow arbitrary boundary layer bleed to exist on any of the solid surfaces. The boundary layer bleed is specified in terms of outflow velocity at each selected node point on the surface grid. This specification of outflow velocity rather than mass flux is consistent with the notion that the outflow mass flux in a real operating inlet with boundary layer bleed is a function of the solution and, therefore, cannot be specified ahead of time. This is because the surface density changes as the location of the inviscid compression process changes.

The OVERFLOW code has been successfully used to describe an application of a Mach 5 inlet to a waverider (Reference 37) flowfield. Examples of this application showing the complexity that can be simulated easily with OVERFLOW are given in Figures 6 through 10. Figure 2 showed the centerplane grid used, while Figure 6 shows the centerplane Mach number distribution. Sample characteristics of the complex, three-dimensional internal flow (Figure 7) are shown in Figure 8. This inlet uses a much-discussed "bypass duct" in order to eliminate the sidewall vorticity and low-momentum features typical of those found numerically and experimentally in the original Mach 5 inlet design. This solution represents the height of an inlet designer's desire in terms of the ability to analyze a given set of complex internal flow contours subject to various prescribed bleed situations located at various places in the inlet. Typical turnaround times for this code for a million nodes are less than two days, extremely rapid when compared with two to three weeks for the same problem with SCRAM3D.

V. EXAMPLES OF DESIGN AND REDESIGN USING MODERN CFD

V.1 The "Mach 10" Inlet

During the course of the NASP program, several variants of the engine inlet flow path, up to design "E-25," were put forth. These designs for the NASP inlet system were very simplistic ("cartoon") realizations of a desired compression process. The length of the NASP inlet was excessive because of the continued desire to have either fixed geometry or minimally-variant geometry scheduled with Mach number for the inlet. Under the NASA Generic Hypersonics Initiative, efforts under the current Grant were guided to the extension of the design philosophy used in the "Mach 5 inlet" to design a better "Mach 10 inlet," and then the NASP inlet scheduled for Mach 10 operation could be compared directly with the detailed design of a "real" Mach 10 inlet. The NASP program virtually never came to grips with the reality that their inlet would require boundary layer bleed to achieve the desired efficiencies through the lower Mach number range. For example, the NASP E-21 inlet had recoveries at Mach 5 in the order of 25 to 30%. This is in contrast with the stated requirement of the NASP program to have an inlet whose recovery was approximately 50%. The reader might recall that the "Mach 5 inlet" was designed for (and produced actual experimental) recoveries of between 45 and 50%. The new "Mach 10 inlet," of course, would require boundary layer bleed to operate through the lower Mach number regions, but could not operate with boundary layer bleed beyond Mach numbers of about 6 due to the thermal loading.

For purposes of the design of a Mach 10 inlet, a geometry similar to the Mach 5 multiple-ramp, two-dimensional inlet was assumed. This presented a flowfield at the cowl lip that was a

constant Mach number and had the thick boundary layer associated with the ramp flowfield. The inherently simple flowfield developed by using articulated forebody ramps, easily schedulable to Mach number variations, was chosen in the Mach 10 design. Figure 9 shows a simple "cartoon" inlet for a Mach 10 flow. The flow solution for this inlet is shown in Figure 10. Our Mach 10 design evolved from this straight-walled inlet. Again, in the Mach 10 design case, various non-focusing compression surfaces were invoked in the internal flow portion to minimize the length, and therefore weight, of the hypothetical inlet system. Detailed results from this design study are discussed in Reference 8 and the final contours (shown to a highly-exaggerated vertical scale) and flowfield solution for one on-design Mach 10 case are shown in Figure 11. The final design contours shown in Figure 11 are the result of a lengthy design process involving the use of the SCRAM2D FNS code. The inlet geometry was then extended to three dimensions in order to investigate the flow quality of the inlet subject to the sidewall's viscous effect. The basic inlet discussed here has a total inviscid turning angle of 36 degrees. This turning angle, at Mach 10, is sufficient to produce a very high pressure ratio. Average calculated pressure ratios for variants of the inlet discussed here are between 100 and 150.

The process of design in an internal flow system, with all of its attendant elliptic behavior is much like laying a piece of linoleum that is slightly too large for the space: you step on it in one place, it pops up in another. By analogy, when the compression is relaxed in one place, it increases in another, resulting in an increased adverse pressure gradient and attendant boundary layer separation problems. By way of example to demonstrate the process involved with the man-

in-the-loop design used to arrive at the contours shown in Figure 11, notes concerning the various modifications (up to Mod. 26) to obtain an acceptable design are given below.

Mod. 1 A full inlet forebody was introduced to an old Mod. 14, version 1 of a preliminary wind tunnel model design study to develop the contours for a flight case. The boundary layer along ramp due to forebody was thicker at the ramp shoulder than in the old Mod. 14, causing cowl lip shock to impinge on the boundary layer upstream of the shoulder. Reflected shock pattern intensified. Cowl was then pulled back so that shock pressure rise occurred near the shoulder, and this reduced reflected shock strength. Ramp shocks coalesced early, and the boundary layer became thicker. Adverse cowl and ramp surface pressures ensued within throat region.

Mod. 2 Angle of attack was increased from 0 to 10 degrees. Early shock coalescence persisted. Ramp boundary layer occupies large part of the throat region and separates from the ramp shoulder, but remains attached on the cowl.

Mod. 3 Because the ramp shocks coalesced prematurely and the ramp boundary layer occupied most of the throat region, the forebody was extended and the throat region widened. The resulting ramp shocks were realigned. Due to the widening of the throat, however, the shock from the cowl lip now hits downstream of the shoulder, and the reflected shock escapes through the rear of the inlet.

Mod. 4 To counteract the cowl lip shock and cowl expansion, a number of geometry changes were made. The shoulder was slid further downstream along the second ramp to meet the cowl shock. The throat width became narrower in the process. The section past the shoulder was also extended, and the cowl "blip" moved further downstream. This resulted in reasonably even pressure distributions along the ramp and cowl within the region after an optimal cowl starting point was found.

Mod. 5 The cowl and the ramp portion past the shoulder were then turned up to be parallel to the combustor axis. The shoulder was left sharp. Problems with obtaining solutions followed, with the code usually dying at a point in front of the cowl lip.

Mod. 6 The shoulder was then rounded. Separation at the shoulder propagated upstream, suggesting an unstart. Shocks from the ramp coalesced in front of the rotated cowl lip.

Mod. 7 Premature shock coalescence was then eliminated by extending the forebody leading edge. The separation problem at the shoulder persisted however.

Mod. 8 The ramp section past the shoulder was then raised 5 degrees. This eliminated the separation problem present in Mods. 6 and 7. To obtain a 1 : 3 boundary layer thickness to throat width ratio, the transition point was moved downstream. This however resulted in some separation along the ramp at those two points along with

misalignment of the ramp angle shocks. In addition, the reflected cowl shock coming from the ramp was inducing separation along the laminar cowl boundary layer. The surface pressures rise sharply and then lower towards the exit. The overall compression is low.

Mod. 9 The requirements here dictate a level outflow, so the flared ramp section past the shoulder was realigned. This also formed a curve to counteract the expansion past the shoulder. The cowl forward slope section was also made larger to counteract the expansion coming from the cowl lip shock - ramp boundary layer interaction. Compression was higher at the smaller exit. Neither the forward slope of the cowl nor the bend on the ramp past the shoulder appear to have a large effect in counteracting expansions. Separation of the boundary layer along the cowl caused by the reflected cowl lip shock coming from the ramp persists.

Mod. 10 To counteract the expansion past the ramp shoulder more effectively, the bend was moved further downstream. The upward slope on the cowl was followed with a downward slope, forming a blip to counteract the reflected cowl lip shock coming from the ramp. The cowl contour was leveled off at the exit. The reflected cowl lip shock hit forward of the cowl bump and was reflected back to the ramp. The backward slope of the ramp also generated its own shock at its base. The cowl lip shock continually hits forward of the ramp shoulder.

Mod. 11 Compression at the exit was low in Mod. 10 so the exit was narrowed by leveling off the backslope of the cowl bump earlier. This also served to lessen the shock coming from the base of the backslope. The exit pressures were higher.

Mod. 12 The cowl was straightened to provide a baseline solution. This caused lower exit pressure than in Mod. 11. The shock coming from the ramp shoulder was reflected from the straight surface without being weakened. The pressure drop due to the cowl lip shock - boundary layer interaction reaching the cowl surface was more than in Mod. 11.

Mod. 13 To reduce shoulder separation still further the ramp section past the shoulder was angled from 5 to 8 degrees upwards and bent back to be level. The cowl remained straight, and the exit width matched that of Mod. 12. This did not reduce separation however. The pressure distributions were much like those in Mod. 12.

Mod. 14 Since 5 degrees is sufficient to reduce separation, the ramp shoulder angle was restored to that value. The cowl bump was made larger to counteract better the expansion coming from the cowl lip shock - boundary layer interaction. A large separation at the shoulder formed which would probably lead to an unstart.

Mod. 15 The cowl bump was made smaller than in Mod. 14 and larger than in Mod. 11 as a compromise between improving the counteraction of the expansion and preventing a too narrow throat width that leads to an unstart. The inlet did not unstart, but the

reflected cowl lip shock coming from the ramp hit the forward slope of the cowl, and the re-reflected shock was intensified.

Mod. 16 The forward slope curvature of Mod. 15 was preserved in this modification, however the peak was slid down the forward slope so that it would be in position to counteract the reflected cowl lip shock. The backward slope which successfully prevented the shock in Mod. 11 was incorporated here. The bump worked well in counteracting the reflected shock. The transition point along the ramp was then moved upstream. The resulting boundary layer at the throat was thicker (now at 1 : 2.5). The cowl leading edge was moved forward to approach the ramp shock coalescence point. After the changes, the reflected cowl lip shock hit forward of the cowl peak, and the re-reflected shock was intensified.

Mod. 17 To meet the reflected cowl lip shock coming from the ramp, the bump was moved upstream and to counteract the expansion, and the forward slope was increased. However, a shock and an expansion wave parallel to it came from the forward slope of the cowl bump and the cowl peak, respectively, causing more adverse pressure distributions along the ramp surface. Both the ramp and cowl pressure distributions were more adverse than in Mod. 16.

Mod. 18 Starting from Mod. 16, the cowl bump was slid upstream, preserving its geometry, to meet the reflected cowl lip shock. High pressures within the throat region

ensued as a separation at the ramp shoulder propagated upstream suggesting that an unstart was about to take place.

Mod. 19 Beginning again from Mod. 16, the bump was made to peak at a lower upstream position along the slope. The reflected cowl lip shock was counteracted. Both the separation which occurred in Mod. 18 as well as the shock and expansion in Mod. 17 were avoided.

Mod. 20 The backslope was made gentler here. This resulted in a less intense shock coming from its base.

Mod. 21 The bend past the shoulder was moved upstream to better counteract the shoulder expansion. Exit height was narrowed slightly in the process. The overall compression within the throat region was higher. Little advantage was gained however in counteracting the expansion.

Mod. 22 The bend was moved up further, and the exit height was narrowed significantly. The compression was greater than in Mod. 21.

Mod. 23 To provide a baseline solution, the ramp and cowl were straightened. A stronger shock train resulted within the throat region, the pressures becoming higher downstream, causing a number of pressure peaks to form on both surfaces. The initial

peak along the ramp surface, however was less than that of the Mod. 22 and the overall ramp pressure profile was not too much different from that in Mod. 22. The initial pressure drop on the cowl, however was more adverse. The compression near the exit is around 150.

Mod. 24 The ramp section past the shoulder was left straight and the cowl of Mod. 22 was restored. Pressures within the throat region were very high. An unstart at the ramp shoulder began.

Mod. 25 The Mod. 22 ramp section was then restored and the cowl leveled off at the peak. The shock emanating from the cowl surface was stronger than in Mod. 22 where the peak served to counteract it. The pressure profiles along both the cowl and ramp surfaces were more adverse.

Mod. 26 Starting with Mod. 22, to improve the counteraction of the expansion past the ramp shoulder, the bend downstream of the shoulder was continued past the horizontal and then leveled off, forming a bulge-like feature. To maintain the same exit height the bend was made only slight. This served to improve the pressure profile along the ramp noticeably over Mod. 22. The compression near the exit is around 150 as in Mod. 23.

Mod. 26 was carried forward for three-dimensional and off-design computations. Examples of three-dimensional results for this inlet are shown in Figures 12 through 15. Figure 12

shows a comparison between the surface pressure distributions from the 2D and 3D solutions. Figures 13, 14 and 15 show the 3D flowfield in half of the inlet at various streamwise stations. Figure 15 shows the distortion problem typical of this class of inlet. The bypass duct discussed in Figures 7 and 8 represents a viable solution to this problem.

Although the man-in-the-loop design process used here is tedious, it is clear that modern CFD codes can be used to in inlet design. It should also be noted that the contours derived in our Mach 10 inlet design are significantly different from the "cartoon" contours for the NASP inlets and are, in fact, representative of the level of complexity that must exist in the design of a realistic air-breathing inlet system.

V.2 Redesign of an Existing Waverider Inlet

During the course of the NASA Generic Hypersonics program, a Mach 8 hydrocarbon fuel waverider airplane was also under investigation (Reference 38). A simplistic ("cartoon") inlet design using straight surfaces with a sharp shoulder was proposed originally. Molvik performed several calculations using the STUFF and TUFF codes to evaluate the performance of not only the inlet, but of the hydrocarbon combustion system as well. Throughout the course of the present study, the notion of using a sharp ramp shoulder (see Figure 16) to cancel the cowl shockwave (such as proposed in early NASP inlets and this NASA waverider inlet), has been consistently debunked as having no off-design margin in the presence of the thick boundary layers known to exist in these inlets. As a result of the efforts carried out in the present study, in combination with strong recommendations from both NASA-Ames and NASA-Lewis personnel,

the NASP inlet (post E-20) contained a rounded shoulder. The benefits of a rounded shoulder are exhibited for the Mach 8 waverider redesign in Figure 17. The sharp shoulder has no margin against any perturbation in the cowl oblique shockwave location. If, for any reason, the pressure rise effects of the cowl shockwave fall forward of the ramp shoulder expansion, an adverse pressure gradient is created that is not amenable to flow separation control by any practical means. This is because the oblique shockwave is effectively hitting on the forward ramp surface, thus increasing the reflected shock turning angle by upwards of ten degrees. At such high Mach numbers, this is an intolerable situation. The redesigned shoulder largely minimizes this effect while suffering only slight on-design penalties due to the expansion of the ramp boundary layer flowfield ahead of the shock impingement. On the other hand, the inlet has a tremendous off-design Mach number margin, as well as a gust margin, required for an actual flight vehicle. The other primary feature of the redesign is a reduced cowl shockwave strength provided by contouring the cowl surface. The improvement predicted by the OVERFLOW code with the Baldwin-Lomax model is seen in the 2D solutions of Figures 16 and 17. In three dimensions, the merits of the redesign are also seen in Figures 18 and 19. The original inlet is tending toward an unstart, whereas the redesigned one has a steady separation. In the present study, sensitivity of the solutions to the turbulence model in OVERFLOW was examined. Solutions were obtained for the three-dimensional flow in the original and redesigned Mach 8 waverider inlet for both the Baldwin-Lomax and the Baldwin-Barth models. Although the computed flows are different with the Baldwin-Barth model (Figures 20 and 21), switching between the models does not change the requirement to redesign the original inlet. The previously noted tendency of the Baldwin-Lomax model to overpredict separation is quite evident.

V.3 General Comments

Early in this study, combinations of PNS and FNS codes were used to reduce turnaround times by solving the forebody flows (without elliptic behavior) with PNS codes and reserving the FNS codes (SCRAM) for the internal flow portion of the inlet. This is still a viable approach, but may be less useful when the much-faster OVERFLOW or TUFF FNS codes are used. This is because there is a serious "overhead" effort required to make the outflow/inflow link between PNS and FNS codes. For example, it might be easier and faster to choose a variable-density grid for the OVERFLOW code that resolves the important parts of the forebody flow and simply to calculate the entire flow each solution. This luxury results from the inherently-short turnaround time for this modern code. This entire FNS technique was used in the later parts of the present study.

Both the Mach 10 design and the Mach 8 waverider redesign involve the use of modern CFD codes (SCRAM3D, UPS, STUFF, TUFF and OVERFLOW) in a "man-in-the-loop" design process. The redesign took a minimal amount of effort, amounting to only about 10 to 15 full CFD simulations, in order to achieve the desired inlet characteristics. On the other hand, the basic "Mach 10 inlet" design required well over 100 runs, some of which were, of course, short because the UPS and STUFF codes were used. A computerized, automatic design is a very interesting proposition to anyone who has gone through one (or more!) of the man-in-the-loop versions of inlet design.

VI. AUTOMATIC DESIGN

During the course of the present study, an automatic design effort was carried out to support ongoing work under a concurrent NASA program to examine the potential use of an optimizer code (NPSOL) (Reference 17)) for use in determining an optimal three-ramp/centerbody inlet design. A driver code was written that couples the space-marched STUFF code with the optimizer code to design only the multiple-ramp section of an inlet. The goal function for this driver was to achieve a "shock-on-cowl-lip" design, represented by having the three ramp shockwaves intersect at a single point in the flowfield. In addition, among the constraints imposed was to have non-zero ramp lengths, disallowing that class of trivial solutions (several unexpected solutions were obtained from the machine design in the course of the present study). The automated code has the capability to examine the flowfield, modify the ramp angles and origins, recompute the flowfield and examine the goodness of the design, all to produce an optimized three-ramp arrangement. The efforts carried out under the present study were minimal, but indicate the possibility for machine design to alleviate much of the repetitive and tedious efforts involved in man-in-the-loop design procedures.

VII. CONCLUDING REMARKS

Over the past seven years, efforts under the present Grant have been aimed at being able to apply modern Computational Fluid Dynamics to the design of high-speed engine inlets. In this report, a review of previous design capabilities (prior to the advent of functioning CFD) was presented and the example of the NASA "Mach 5 inlet" design was given as the premier example of the historical approach to inlet design. The philosophy used in the Mach 5 inlet design was carried forward in the present study, in which CFD was used to design a new Mach 10 inlet. An example of an inlet redesign was also shown. These latter efforts were carried out using today's state-of-the-art, full computational fluid dynamics codes applied in an iterative man-in-the-loop technique. The potential usefulness of an automated machine design capability using an optimizer code was also discussed. This report finalizes the efforts carried out under NASA Cooperative Grant NCC-507.

VIII. REFERENCES

1. Semi-Annual Status Report, Numerical Investigations in Three-Dimensional Internal Flows; NCC 2-507. 1 October 1987 through 31 March 1988.

2. Semi-Annual Status Report, Numerical Investigations in Three-Dimensional Internal Flows; NCC 2-507. 1 April 1988 through 30 September 1988.

3. Semi-Annual Status Report, Numerical Investigations in Three-Dimensional Internal Flows; NCC 2-507. 1 January 1989 through 30 June 1989.

4. Semi-Annual Status Report, Numerical Investigations in Three-Dimensional Internal Flows; NCC 2-507. 1 July 1989 through 31 December 1989.

5. Semi-Annual Status Report, Numerical Investigations in Three-Dimensional Internal Flows; NCC 2-507. 1 January 1990 through 30 June 1990.

6. Semi-Annual Status Report, Numerical Investigations in Three-Dimensional Internal Flows; NCC 2-507. 1 July 1990 through 31 December 1990.

7. Semi-Annual Status Report, Numerical Investigations in Three-Dimensional Internal Flows; NCC 2-507. 1 January 1991 through 30 June 1991.

8. Semi-Annual Status Report, Numerical Investigations in Three-Dimensional Internal Flows; NCC 2-507. 1 July 1991 through 31 December 1991.

9. Semi-Annual Status Report, Numerical Investigations in Three-Dimensional Internal Flows; NCC 2-507. 1 January 1992 through 30 June 1992.

10. Semi-Annual Status Report, Numerical Investigations in Three-Dimensional Internal Flows; NCC 2-507. 1 July 1992 through 31 December 1992.

11. Semi-Annual Status Report, Numerical Investigations in Three-Dimensional Internal Flows; NCC 2-507. 1 January 1993 through 30 June 1993.

12. Semi-Annual Status Report, Numerical Investigations in Three-Dimensional Internal Flows; NCC 2-507. 1 July 1993 through 31 December 1993.

13. Rose, W.C., Serafini, D.B. and Perkins, E.W.: Innovative Boundary Layer Control Methods in High Speed Inlet Systems. NASA SBIR Phase II Final Report, Contract NAS3-25783, November 1991.

14. Reddy, D.R., Benson, T.J. and Weir, L.J.: Comparison of 3-D Viscous Flow Computations of Mach 5 Inlet with Experimental Data. AIAA Paper 90-0600, January 1990.

15. Kim, Y.-N., Buggeln, R.C. and McDonald, H.: Numerical Analysis of Some Supersonic Viscous Flows Related to Inlet and Nozzle Systems. AIAA Paper 86-1596, June 1986.

16. Rizzetta, D.P.: Numerical Simulation of a Supersonic Inlet. AIAA Paper 91-0128, January 1991.

17. Gil, P., Murray, W., Saunders, M. and Wright, M.: User's Guide for NPSOL: A FORTRAN Package for Nonlinear Programming. Tech. Report SOL86-2, Dept. of Operations Research, Stanford University, 1986.

18. Molvik, G.A. and Merkle, C.L.: A Set of Strongly-Coupled Upwind Algorithms for Computing Flows in Chemical Nonequilibrium. AIAA Paper 89-0199, January 1989.

19. Sorensen, V.L.: Computer Program for Calculating Flow Fields in Supersonic Inlets. TN D-2897, 1965, NASA.

20. Murphy, J.D. and Davies, C.B.: Users Guide - Ames Inlet Boundary Layer Program MK-1. NASA TMX-62, 211, 1973.

21. Syberg, J. and Hickcox, T.E.: Design of a Bleed System for a Mach 3.5 Inlet. NASA CR-2187, 1974.

22. Maslowe, S.A. and Benson, J.L.: Computer Program for the Design and Analysis of Hypersonic Inlets. NASA CR-77749, 1964.

23. Rose, W.C.: A Method for Analyzing the Interaction of an Oblique Shock Wave with a Boundary Layer. NASA TN 6083, 1970.

24. Presley, L.L. and Kutler, P.: Comparison of a Discrete-Shock Finite-Difference Technique and the Method of Characteristics for Calculating Internal Supersonic Flows. NASA paper presented at AIAA Computational Fluid Dynamics Conference (Palm Springs, CA), July 19-24, 1973.

25. MacCormack, R.W.: The Effect of Viscosity in Hypervelocity Impact Cratering. AIAA Paper No. 69-354, April-May 1969.

26. MacCormack, R.W.: Numerical Solution of the Interaction of Shock Wave with a Laminar Boundary Layer. Proceedings of the 2nd International Conference on Numerical Methods in Fluid Dynamics, Lecture Notes in Physics, Vol. 8, Springer-Verlag, 1971.

27. Kumar, A.: Numerical Analysis of the Scramjet Inlet Flow Field Using Two-Dimensional Navier-Stokes Equations. AIAA-81-0185, January 1991.

28. Kumar, A.: Numerical Simulations of Flow Through Scramjet Inlets Using a Three-Dimensional Navier-Stokes Code. AIAA Paper 85-1664, July 1985.

29. Lawrence, S.L., Chaussee, D.S., and Tannehill, J.C.: Application of an Upwind Algorithm to the Three-Dimensional Parabolized Navier-Stokes Equations. AIAA Paper 87-1112-CP.

30. Buning, P.G., Chan, W.M., Renze, K.J., Sondak, D.L., Chiu, I.T. and Slotnick, J.P.: OVERFLOW Users Manual Version 1.6ag. Computational Technology Branch (RFG), NASA-Ames Research Center, June 1993.

31. Perkins, E.W., Rose, W.C. and Horie, G.: Design of a Mach 5 Inlet System Model. NASA CR-3830, August 1984.

32. Prozan, R.D.: Development of a Method of Characteristics Solution for Supersonic Flow of an Ideal, Frozen Equilibrium Reacting Gas Mixture. Lockheed Missile and Space Company, Huntsville Research and Engineering Center, Technical Report LMSC/HREC A782535, April 1966.

33. Steinbrenner, J.P. and Chawner, J.R.: GRIDGEN, Version 9. MDA Engineering, 1994.

34. Wong, M.D.: QUICKGEN Version 1.0 User's Guide (Revised). TN 93-8006-000-47, Sterling Software, May, 1994.

35. Rose, W.C.: Comparison of Solutions to Boundary-Layer and Navier-Stokes Equations for the Case of Mass Removal from a Turbulent Boundary Layer. AIAA Paper 76-150, January 1976.

36. Rose, W.C.: Practical Aspects of Using Navier-Stokes Codes for Predicting Separated Flows. AIAA Paper 76-96, Washington D.C., 1976.

37. Pegg, R.J., et. al.: Design of a Hypersonic Waverider Derived Airplane. AIAA Paper 93-0401, January 1993.

38. Molvik, G.A., Bowles, J.V. and Huynh, L.C.: Analysis of a Hypersonic Research Vehicle with a Hydrocarbon Scramjet Engine. AIAA Paper 93-0509, 1993.

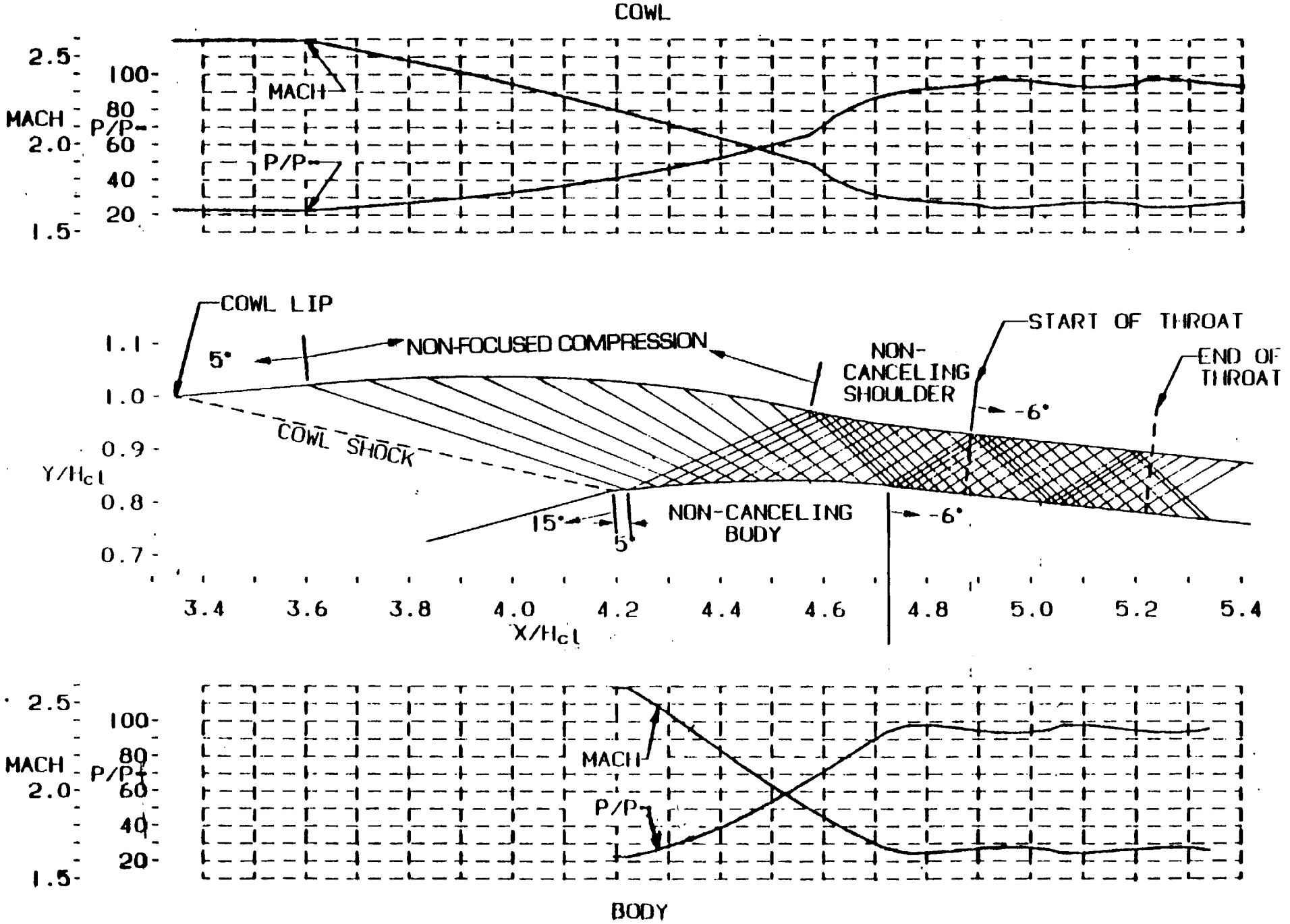

FIGURE 1 **Method of characteristics solution for the Mach 5 inlet at the design condition showing characteristics net for the internal flow.**

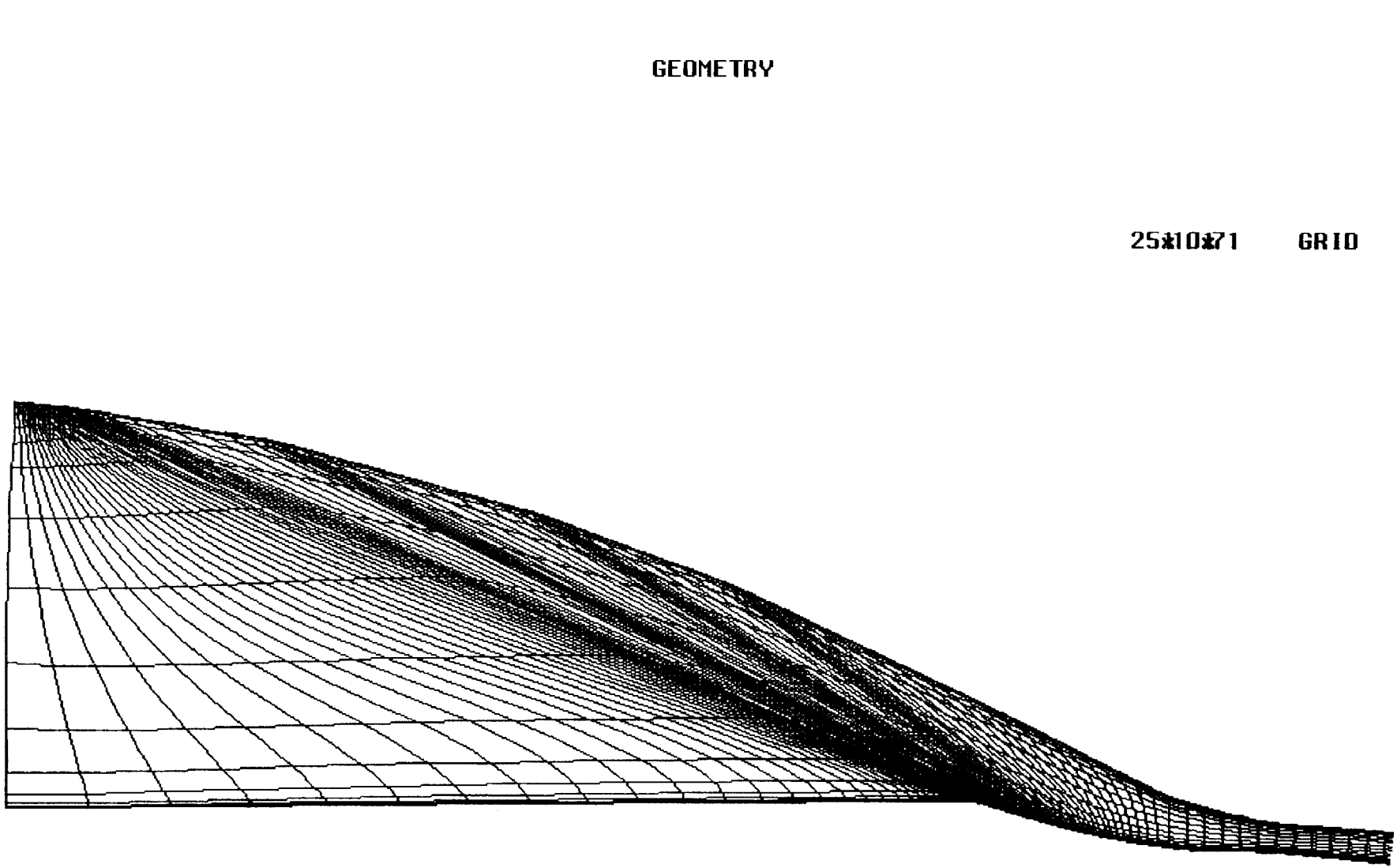

FIGURE 2 **Two-dimensional streamwise grid centerplane for the supersonic outboard module.**

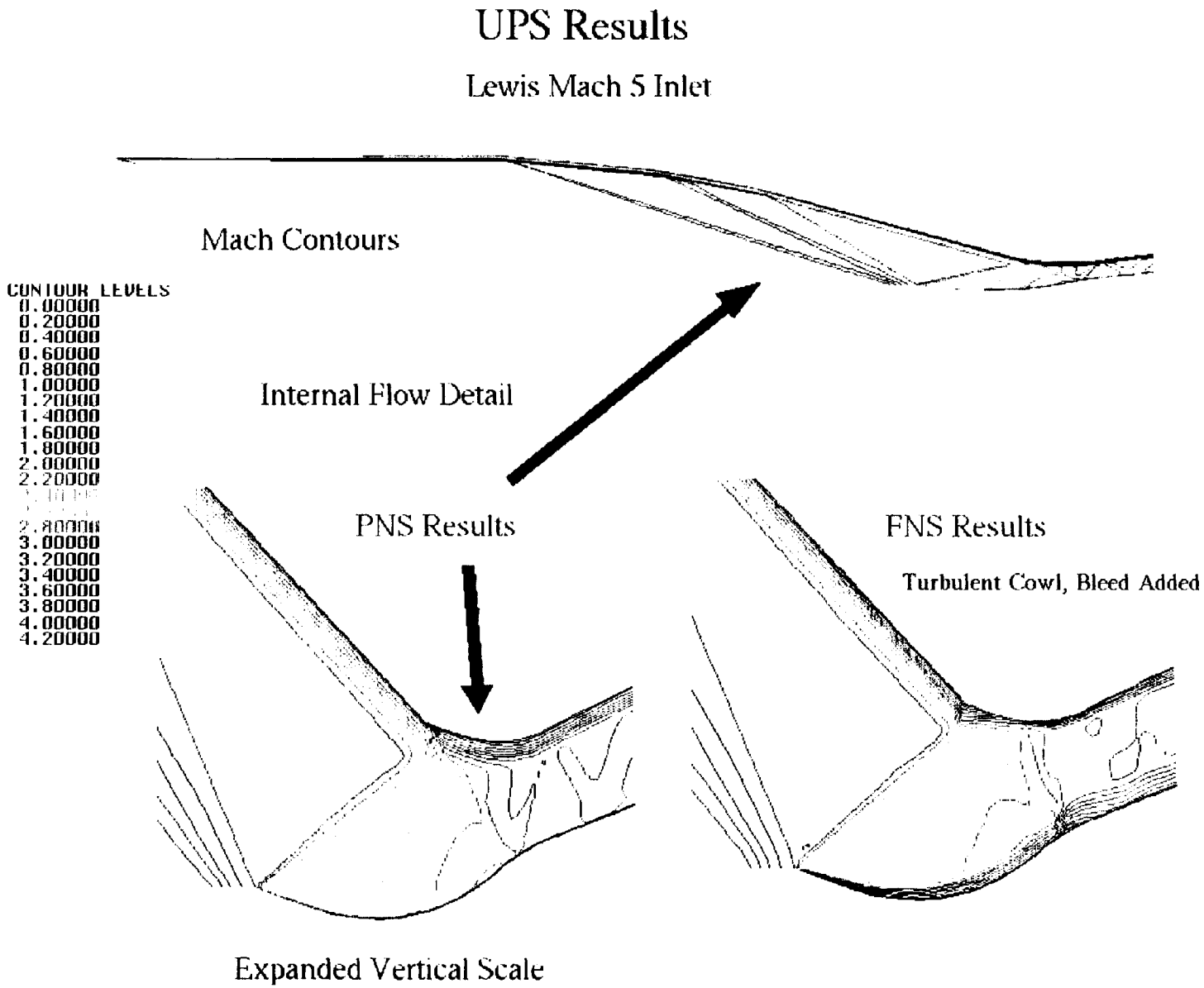

FIGURE 3 **Use of the upstream results from UPS applied as inflow to SCRAM2D code just upstream of cowl lip.**

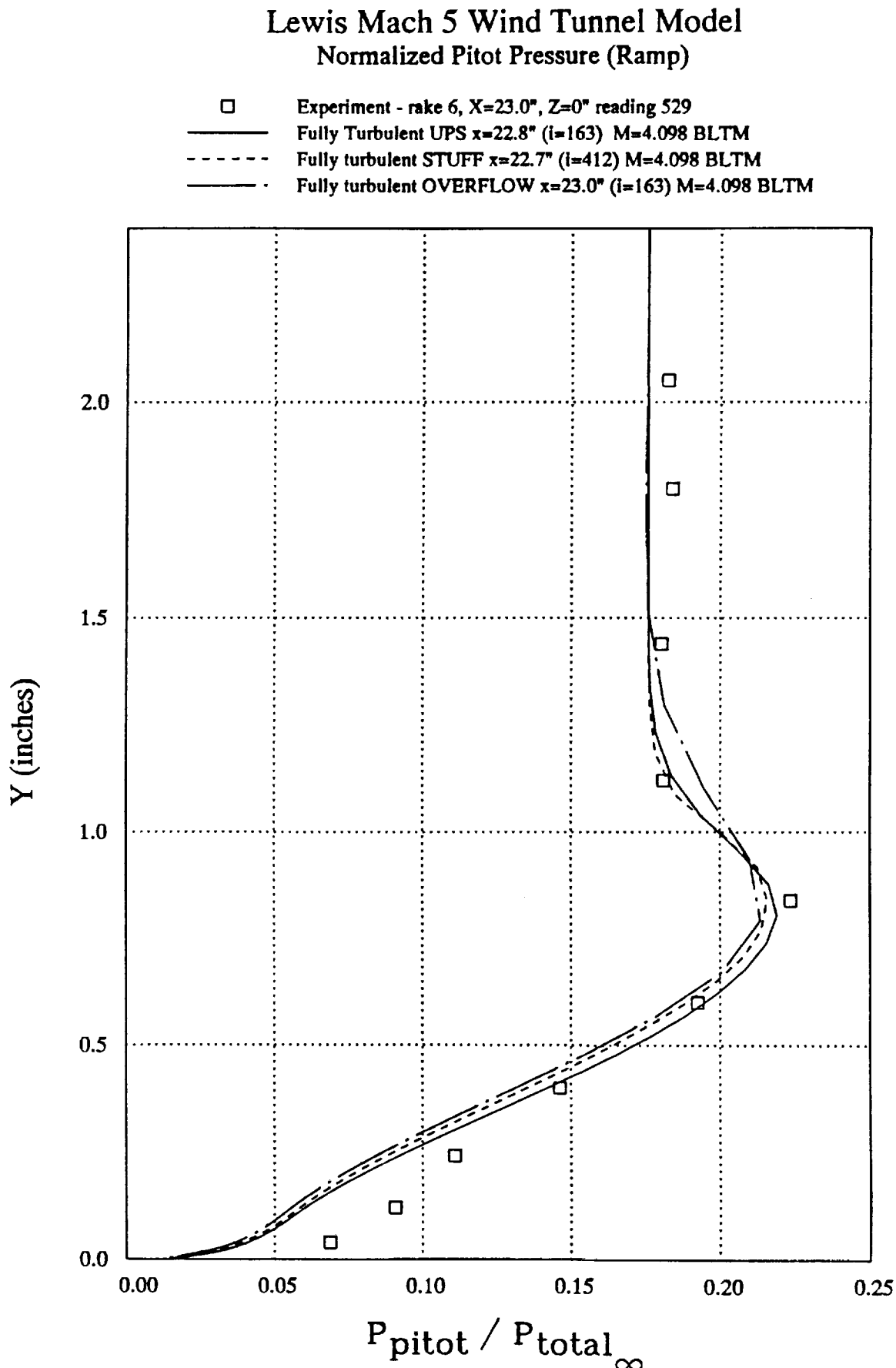

FIGURE 4 **Comparison of results from UPS, STUFF and OVERFLOW with experimental boundary layer/shock wave data from the Mach 5 inlet forebody, rake 6, x = 22.8 in.**

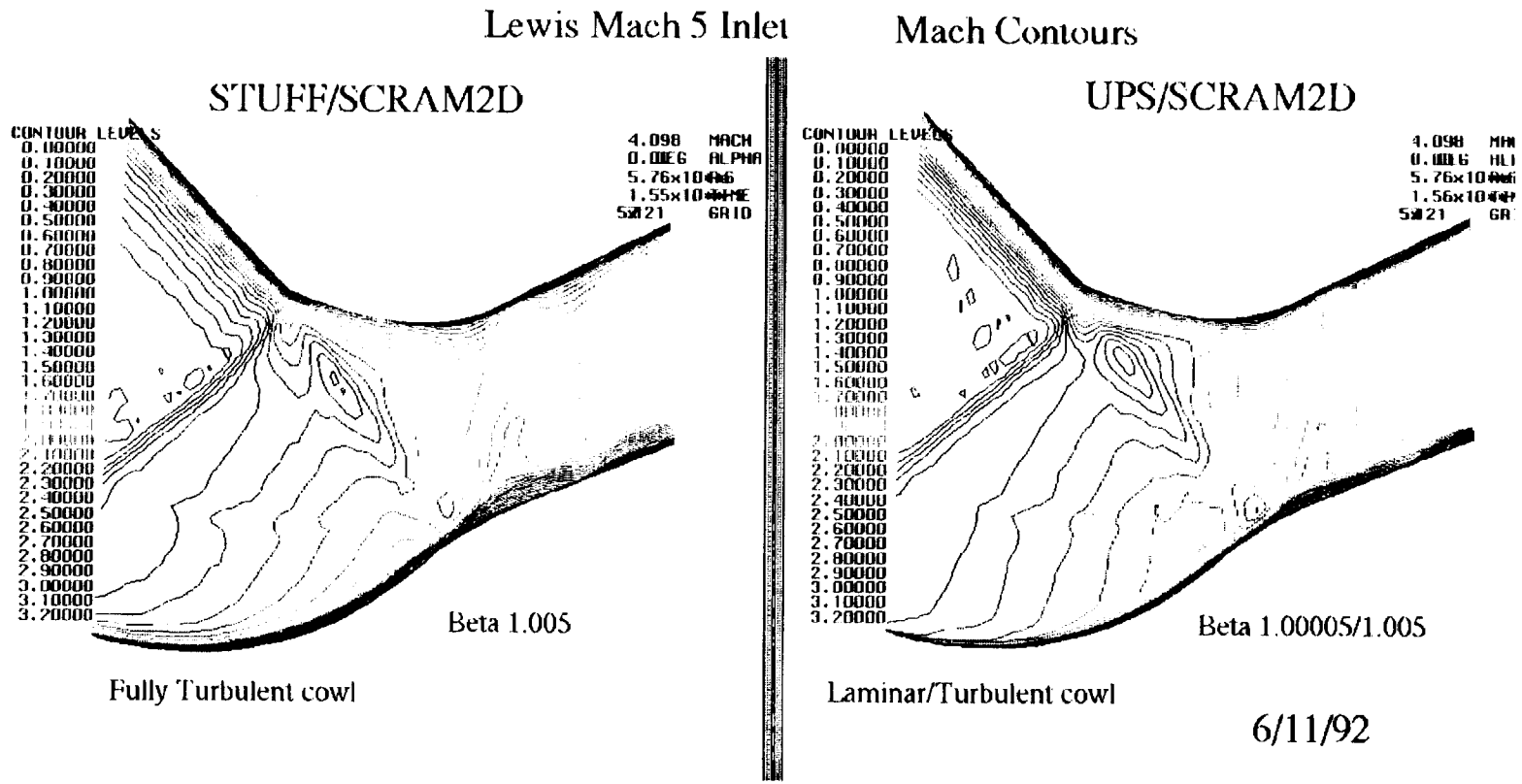

FIGURE 5 **Use of the upstream results from STUFF applied as inflow to SCRAM2D code downstream of cowl lip.**

FIGURE 6 **Outboard module centerplane starting from the origin of the first ramp and ending downstream of the supersonic inlet throat.**

a) **Mach number contours**

Lewis/Langley waverider with full length sidewall/bypass

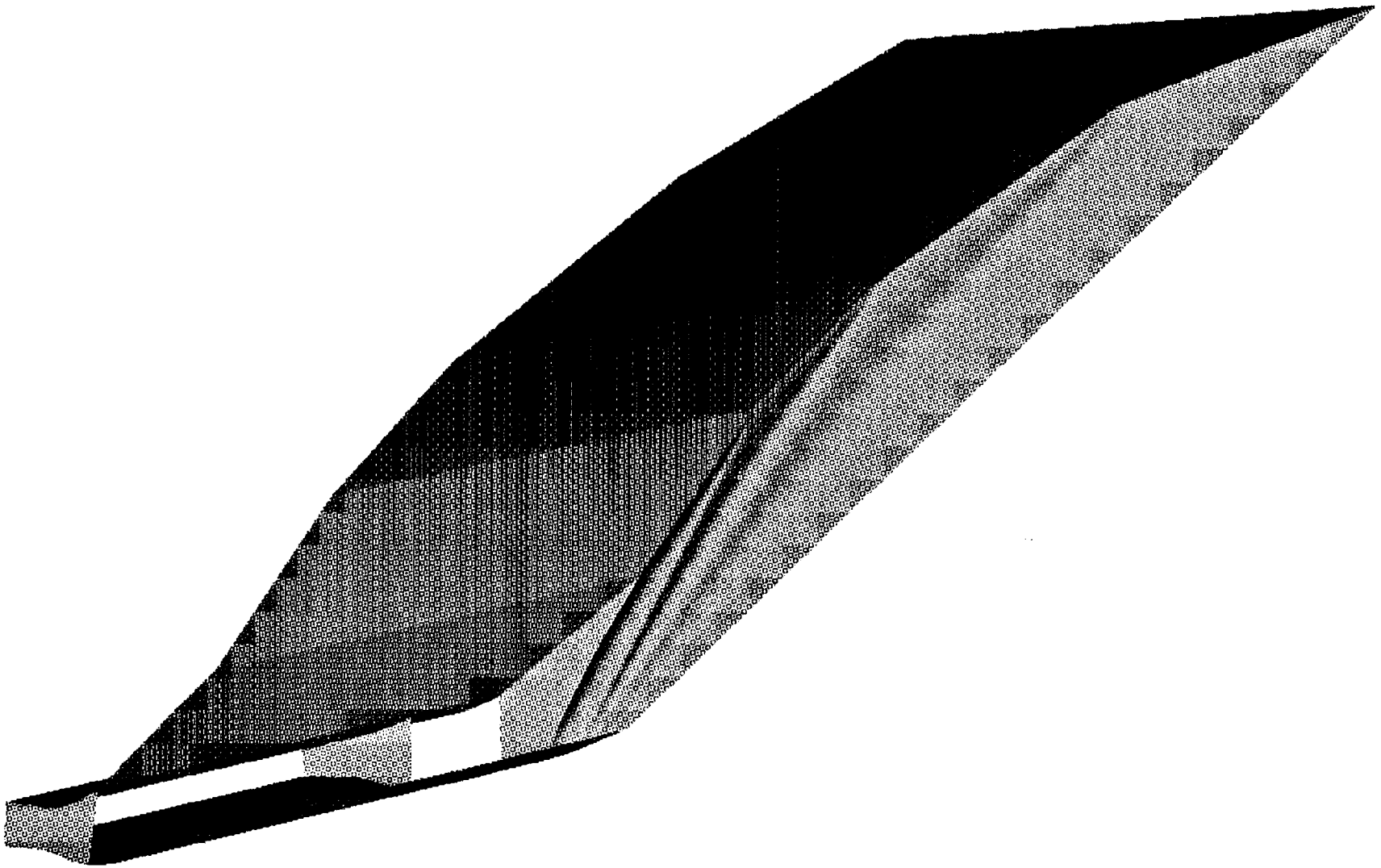

FIGURE 7 **Outboard module geometry with the bypass duct included.**

a) **Entire geometry with very long sidewall shown**

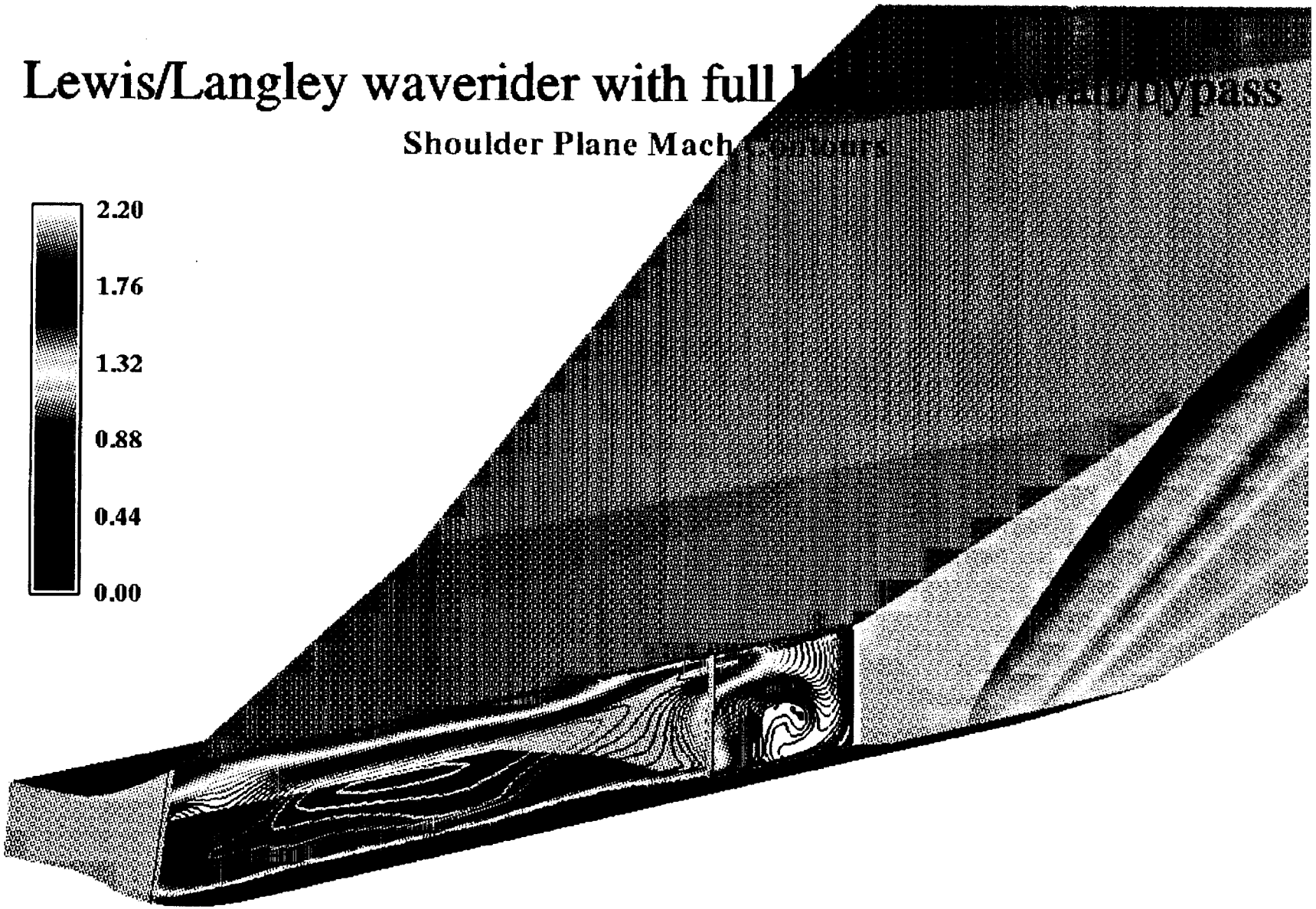

FIGURE 8 **Entire geometry with the crossflow plane at the location where the inlet stream is divided.**

a) **Mach number contours**

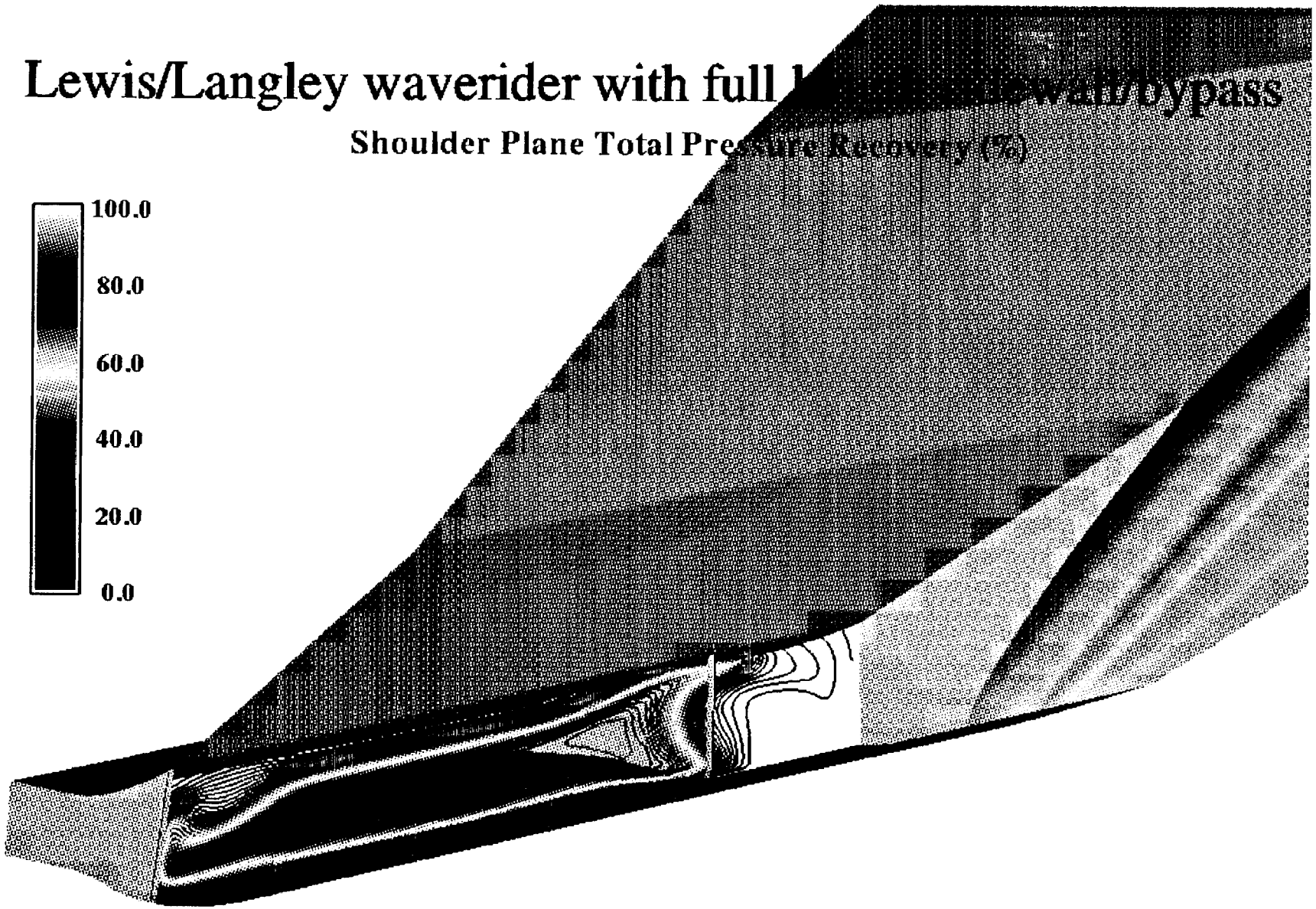

FIGURE 8 **Concluded.**

b) **Normalized stagnation pressure contours**

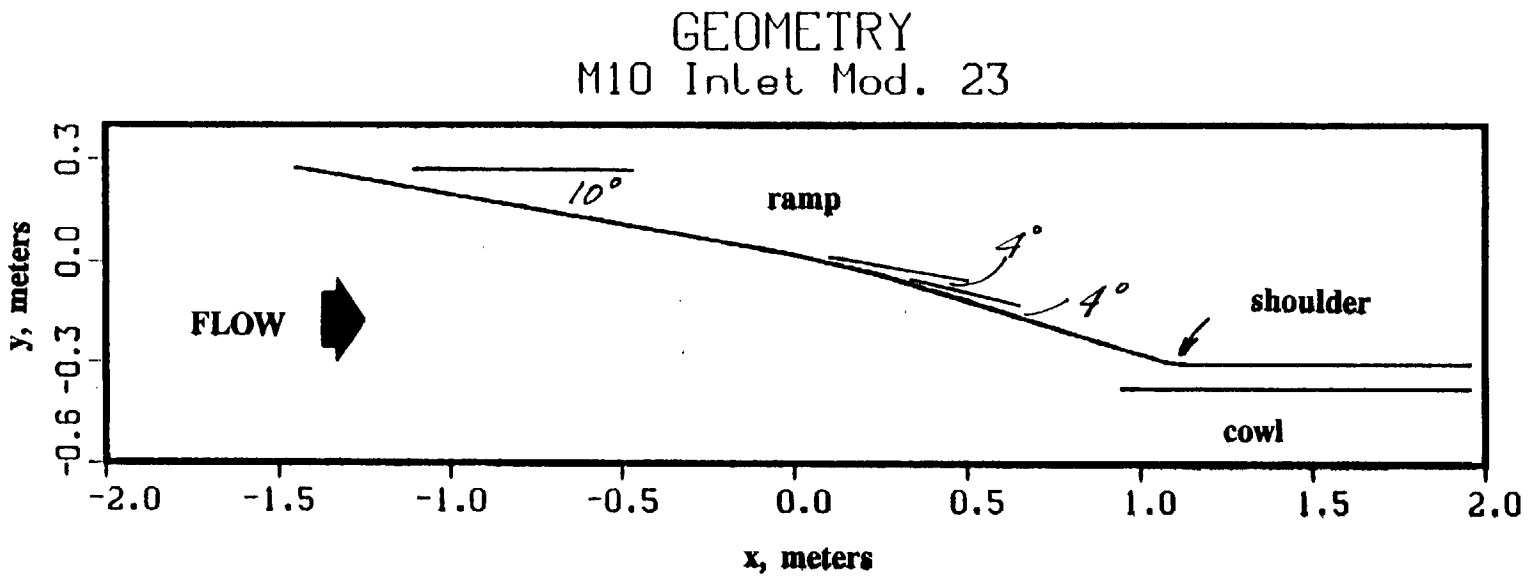

FIGURE 9 **Geometry for 36 degree inlet having a straight cowl and straight ramp.**

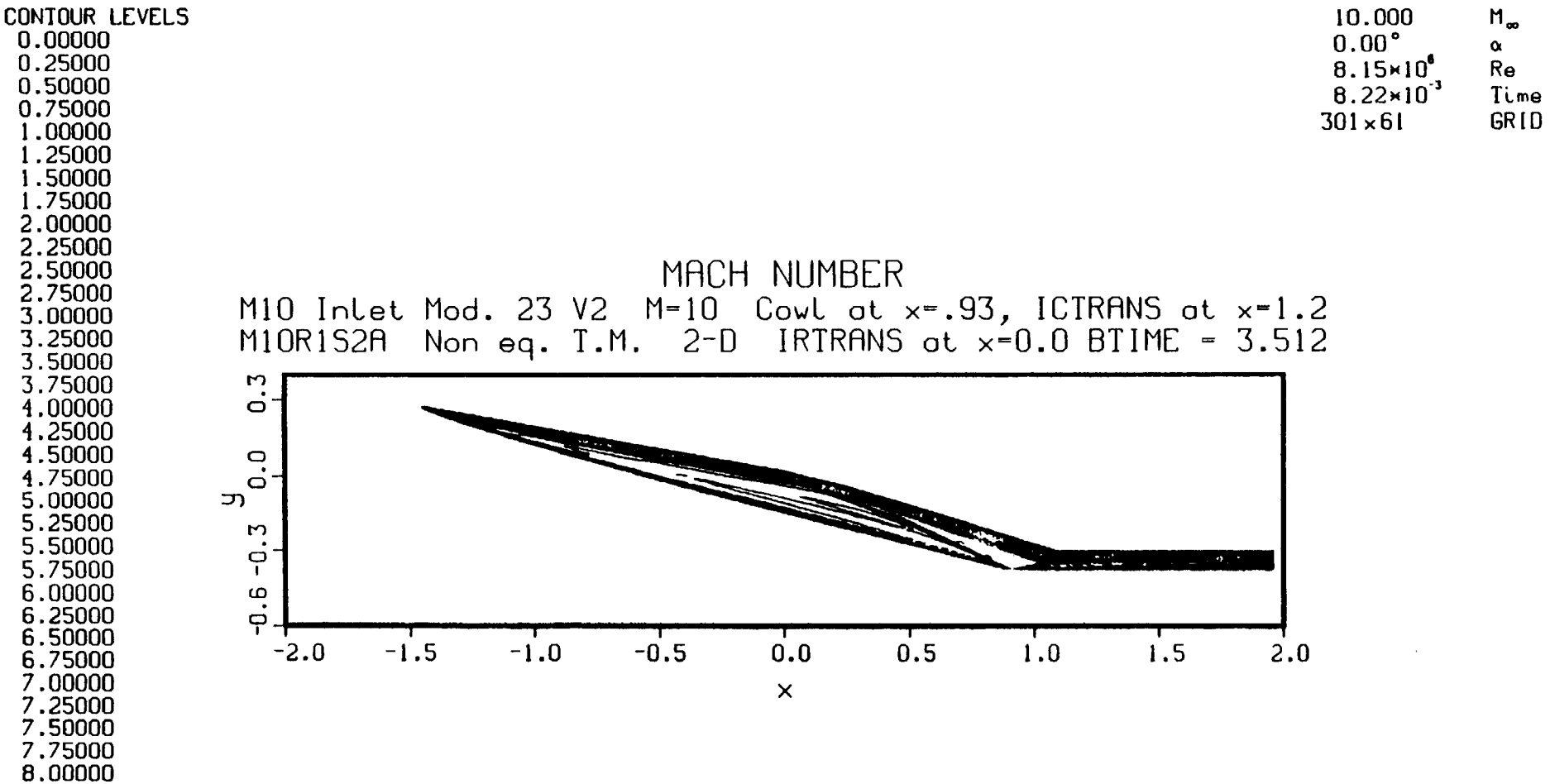

FIGURE 10 **Flow solution for 36 degree inlet with straight ramp and cowl at M=10.**

(a) **Mach number contours shown to correct vertical and streamwise scales.**

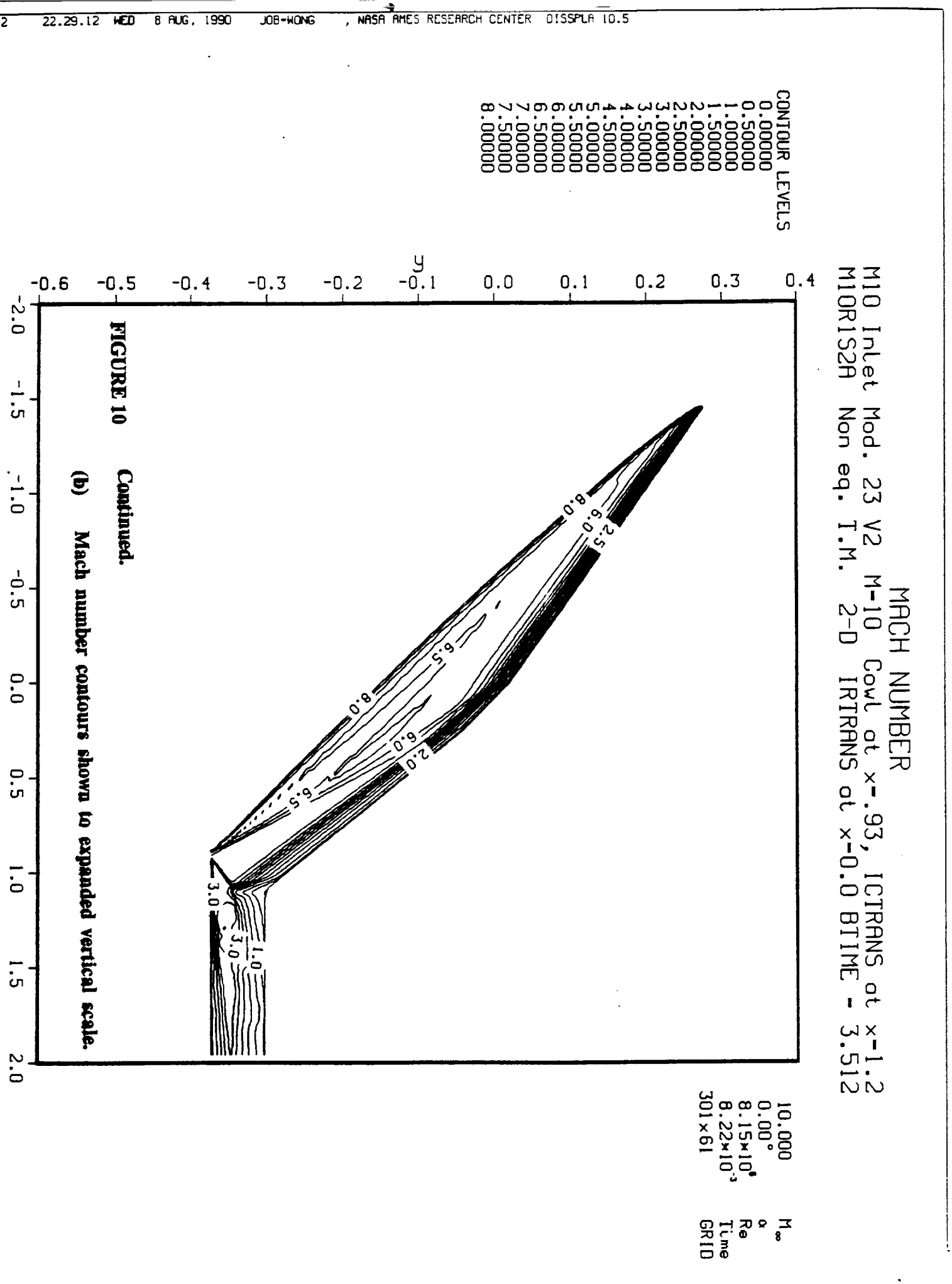

FIGURE 10 Continued.

(b) Mach number contours shown to expanded vertical scale.

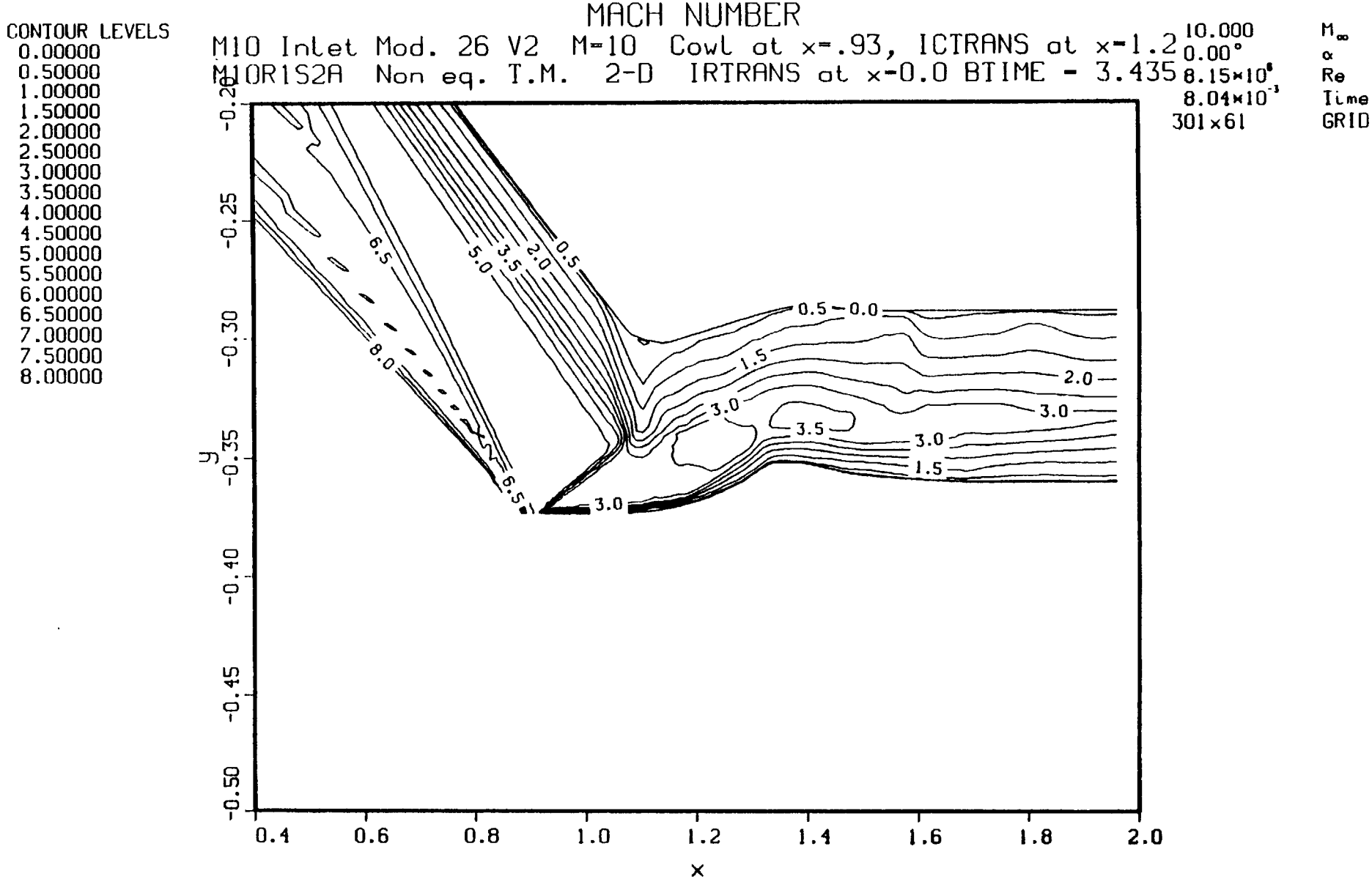

FIGURE 11 **Flow solution for 36 degree inlet with contoured ramp and cowl surfaces at M=10.**

(a) Mach number contour detail in throat region.

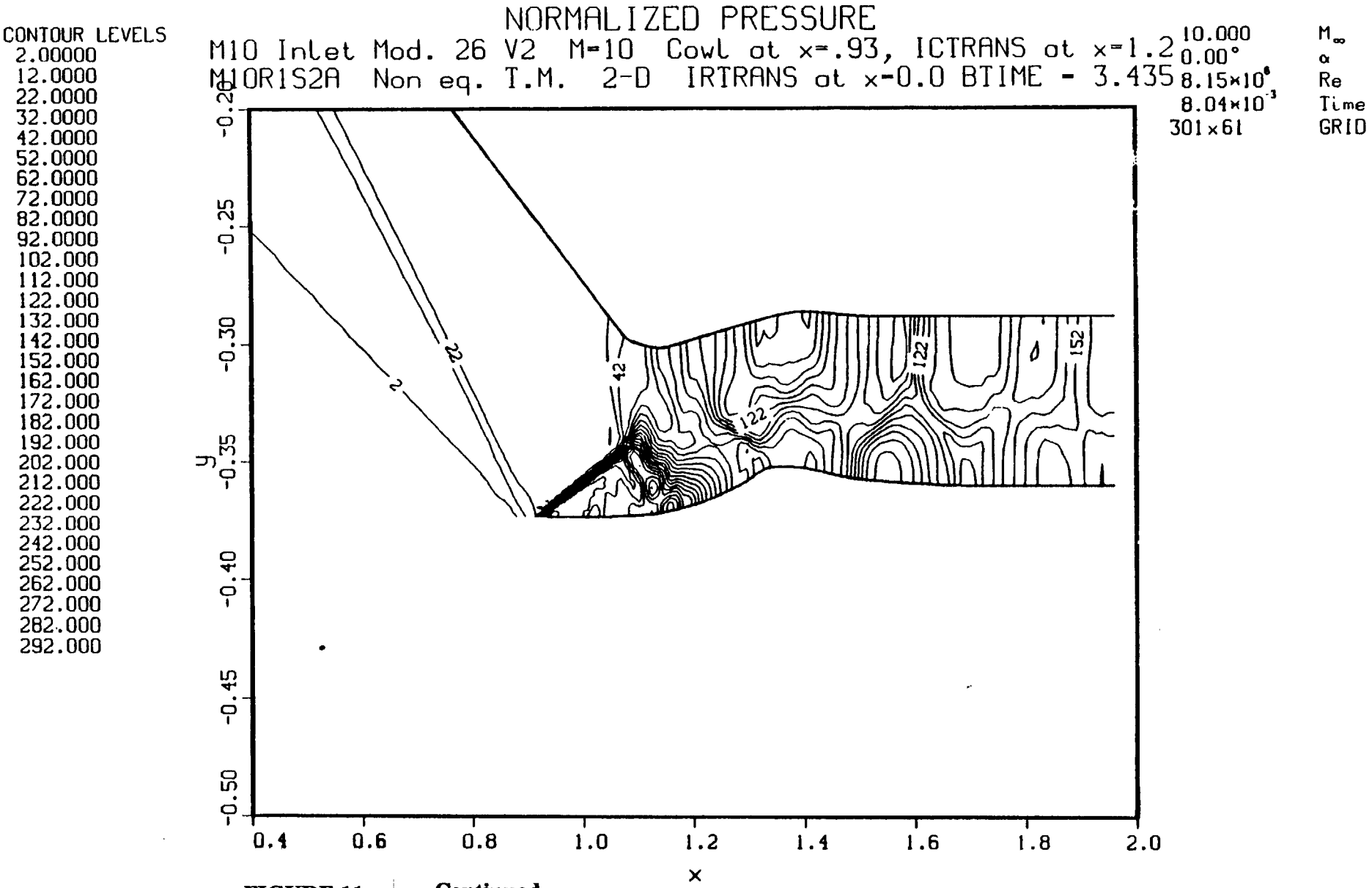

FIGURE 11 **Continued.**

(b) Pressure contours in throat region.

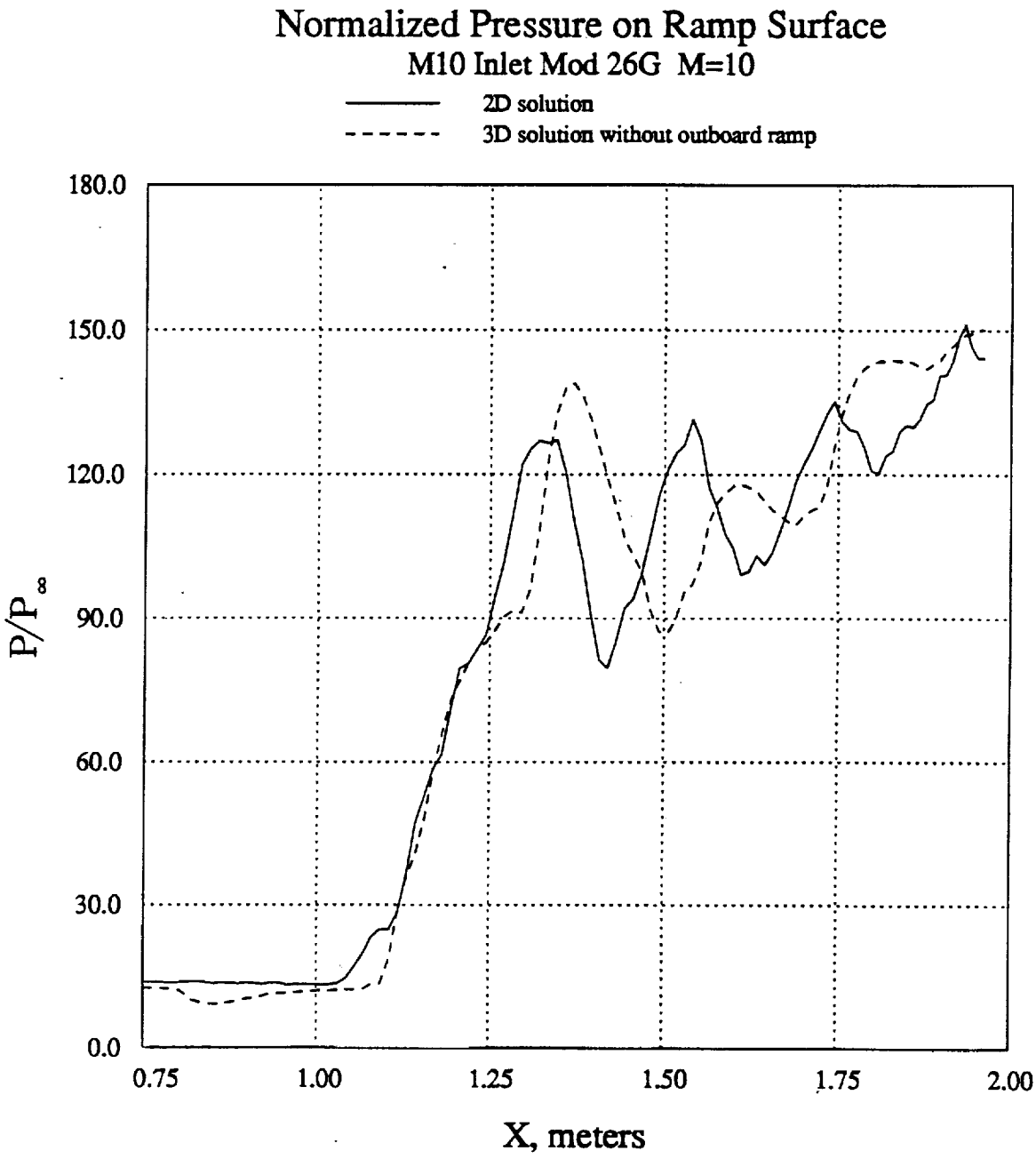

FIGURE 12 Comparison of two-dimensional and three-dimensional (center plane) pressures.

(a) Ramp surface pressure distribution.

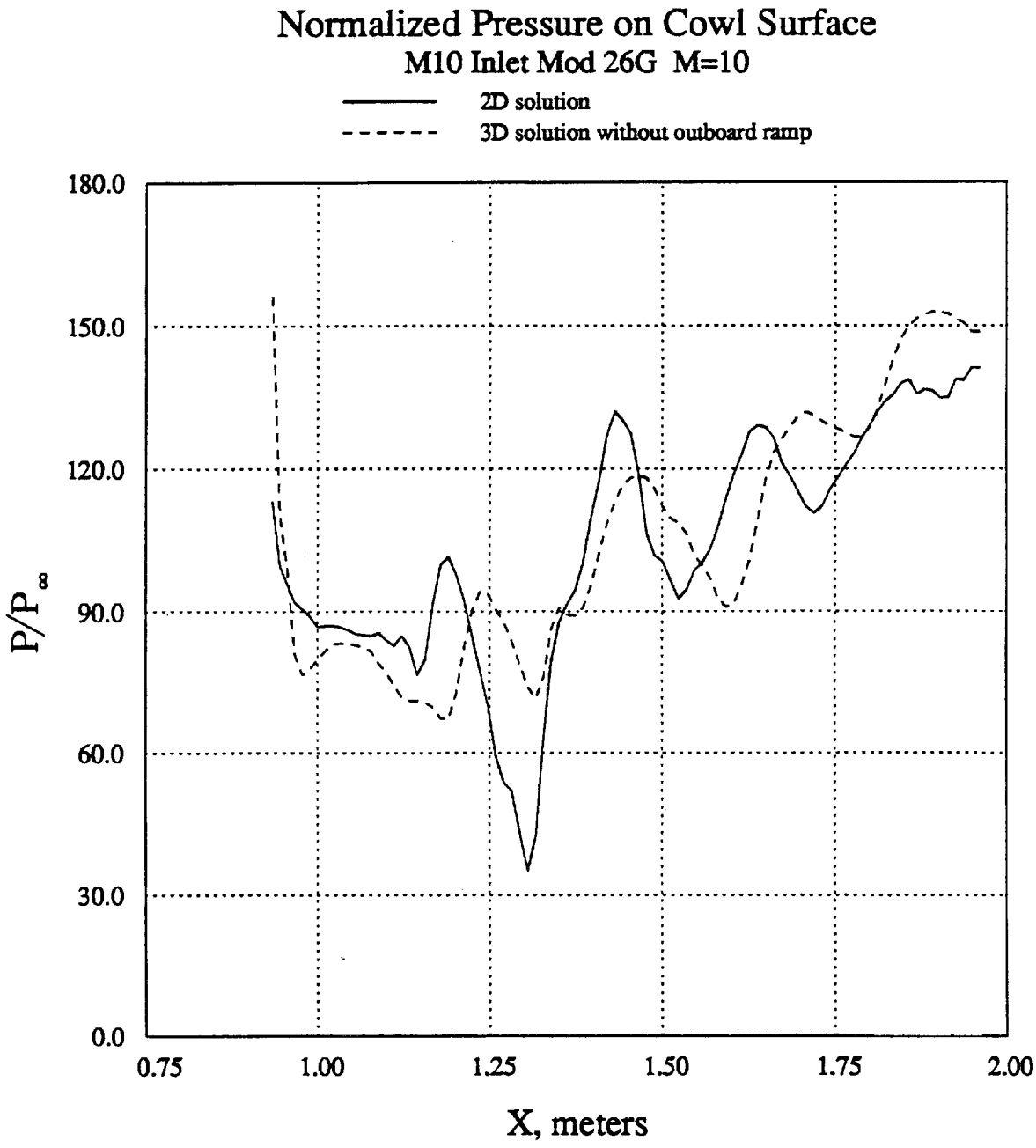

FIGURE 12 Concluded.

(b) Cowl surface pressure distribution.

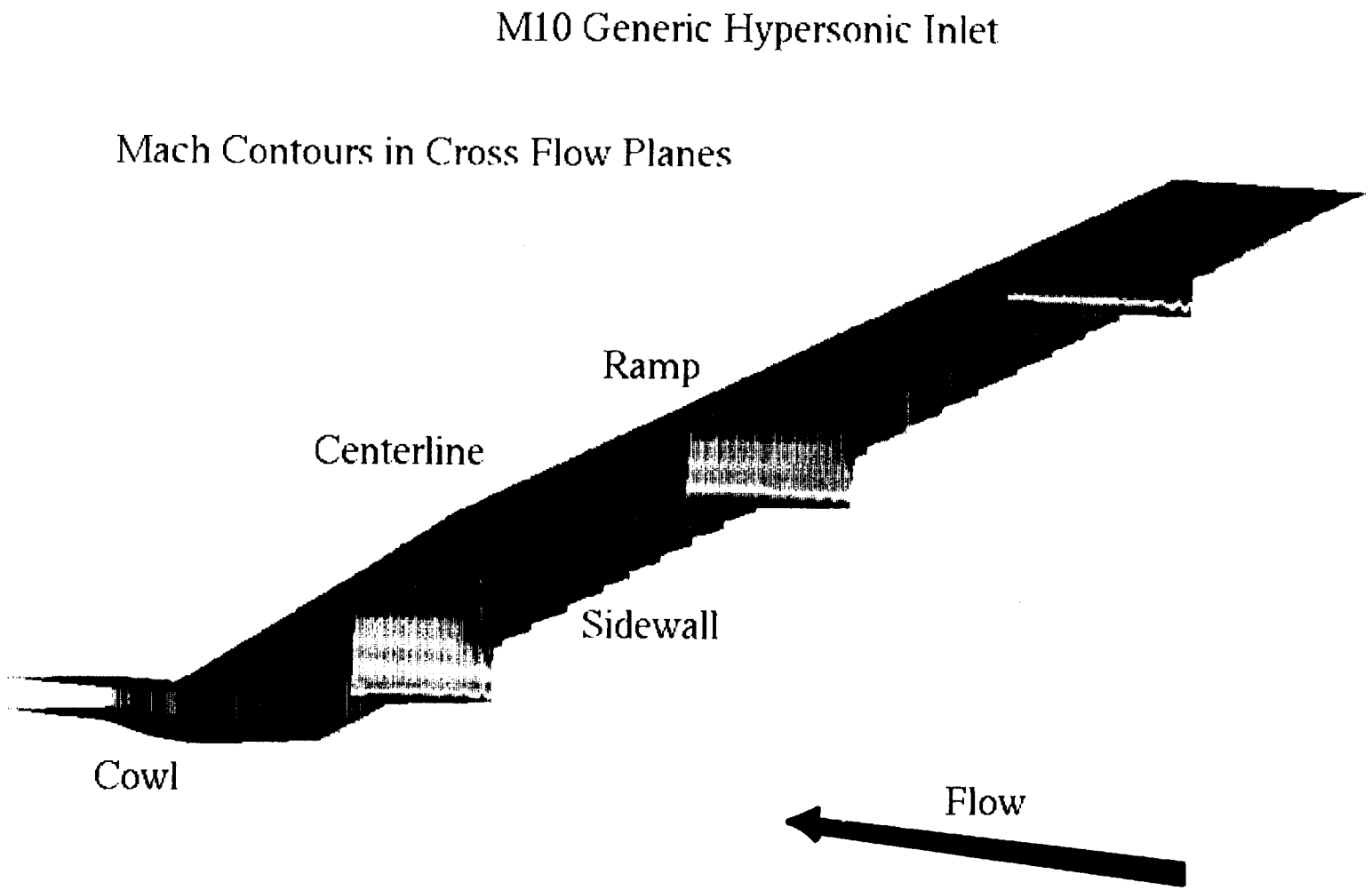

FIGURE 13 **Surfaces used in three-dimensional simulations showing ramp, cowl and swept sidewalls along with Mach number contours in three representative cross flow planes.**

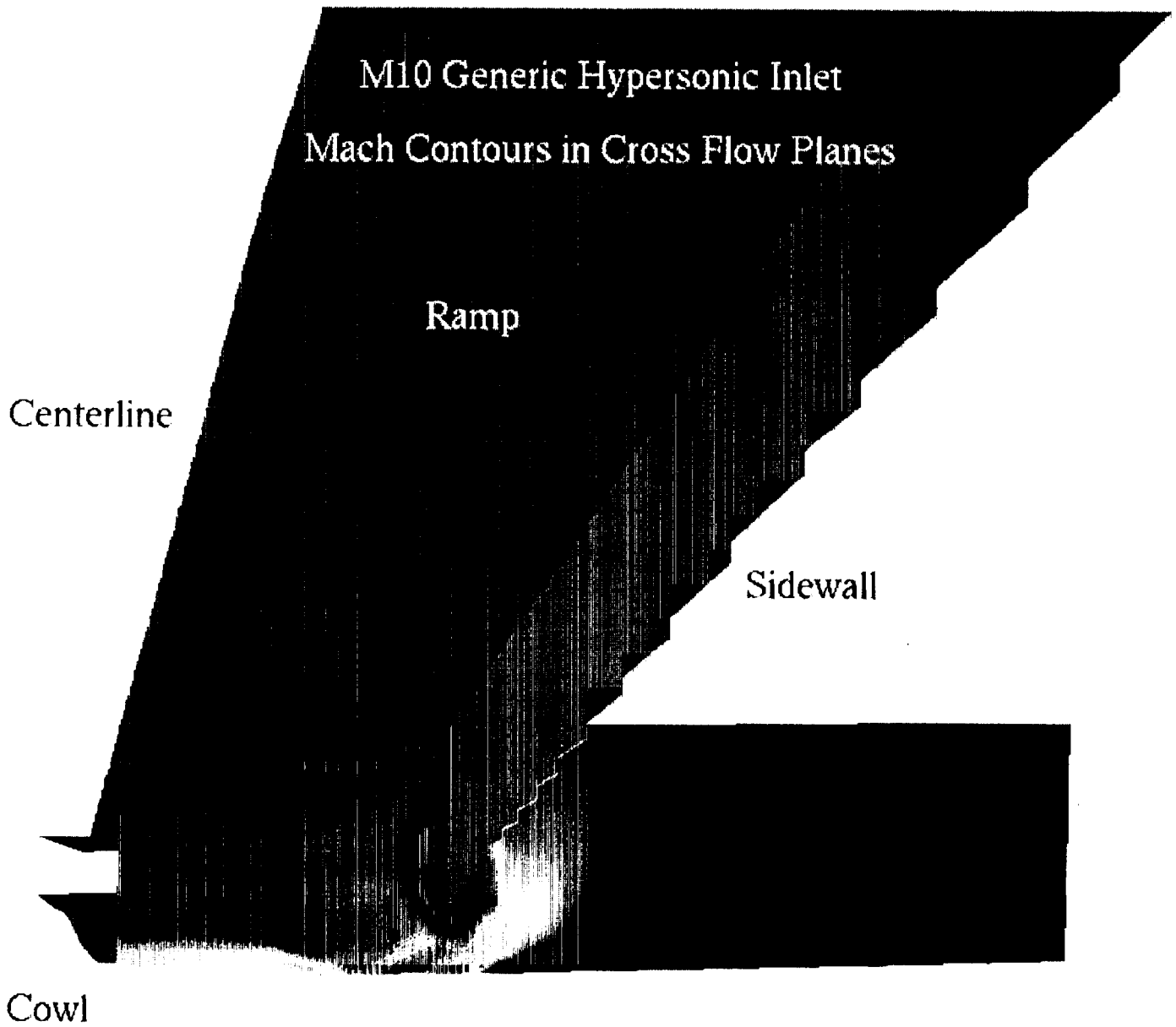

FIGURE 14 **Mach number contours in cross flow plane just ahead of the cowl lip without outboard ramp**

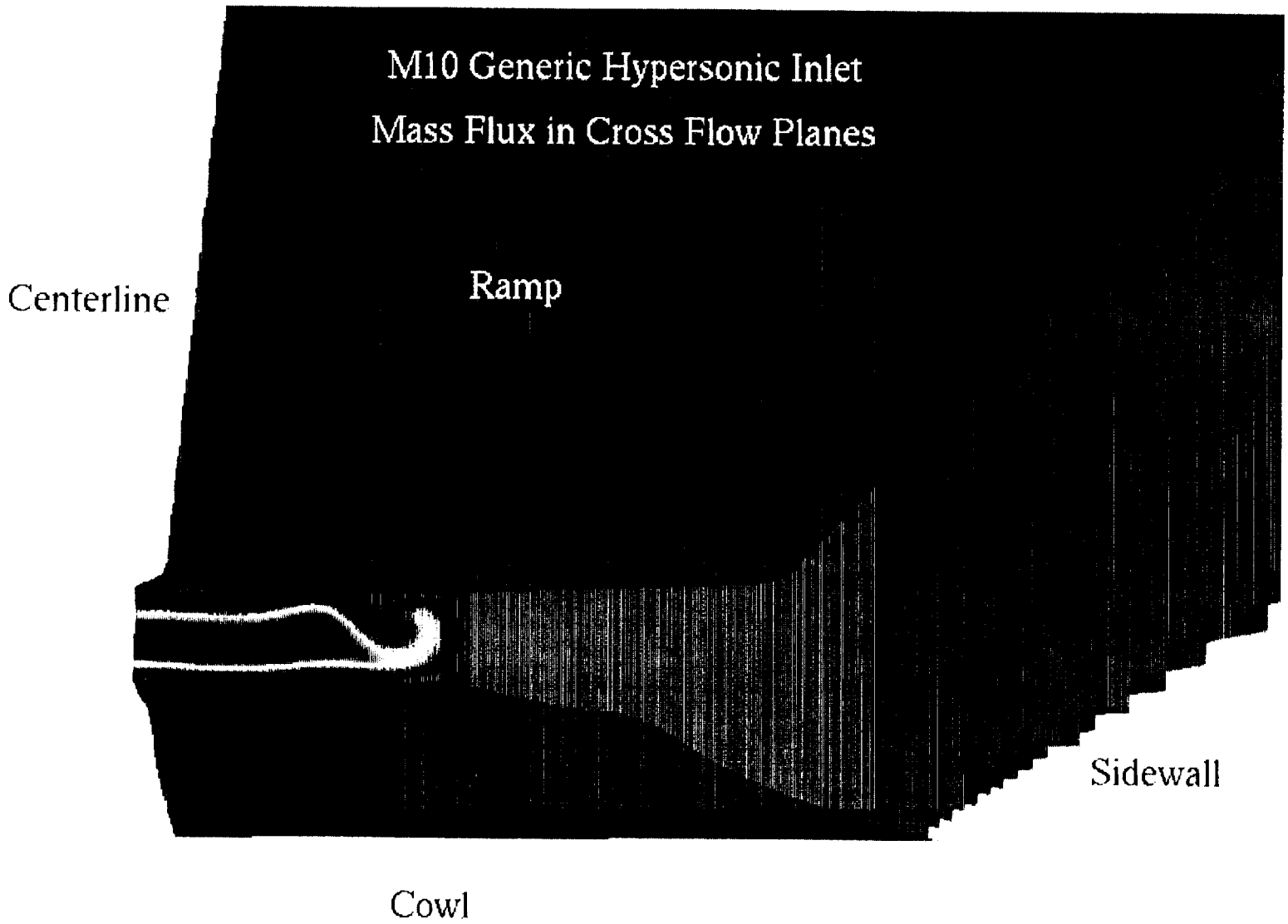

FIGURE 15 Mass flux contour at the exit of the inlet.

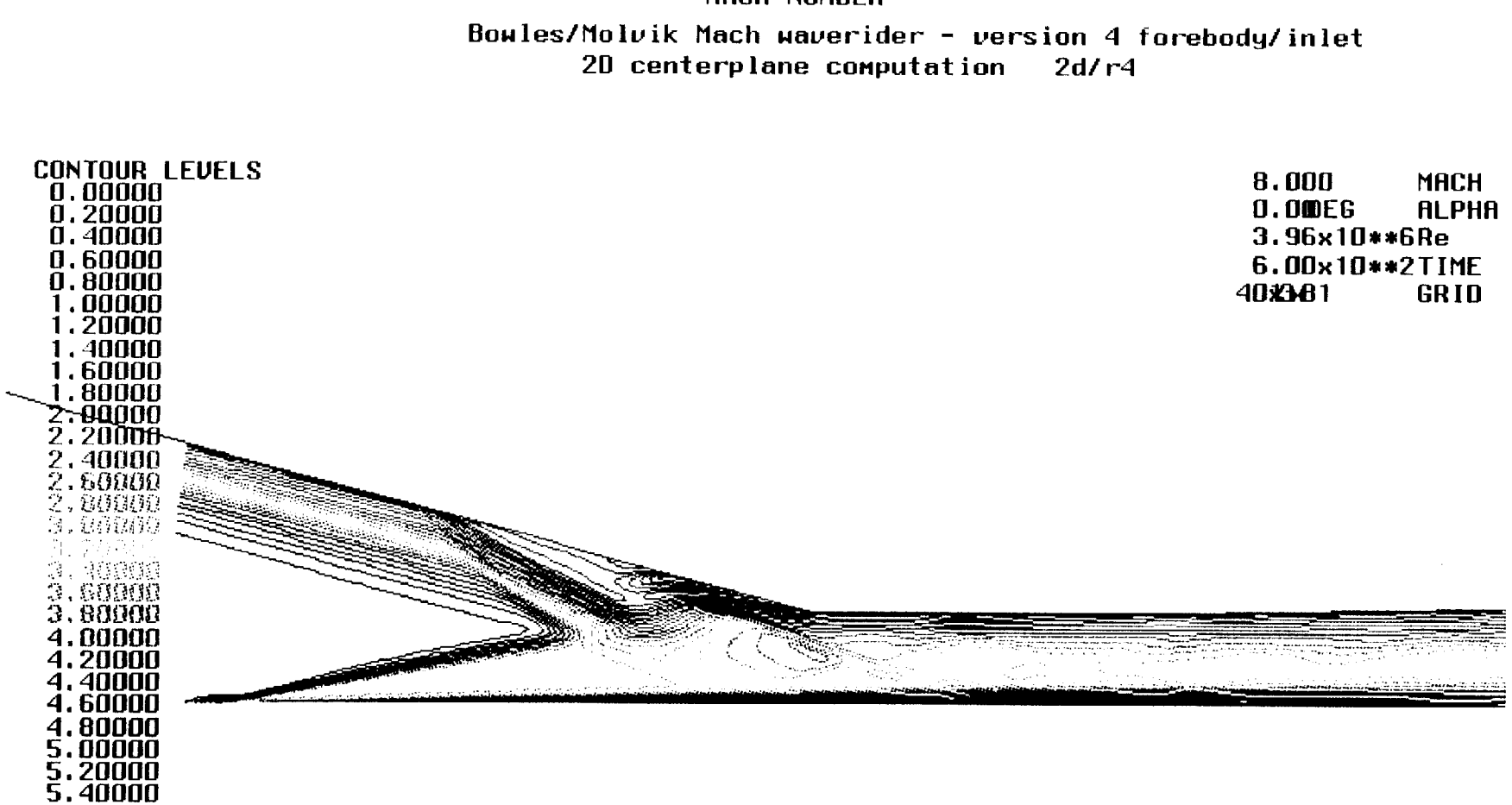

FIGURE 16 **OVERFLOW two-dimensional forebody/inlet solution of the baseline (version 4) inlet at $M_\infty = 8.0$.**

a) **Mach number contours at the centerplane**

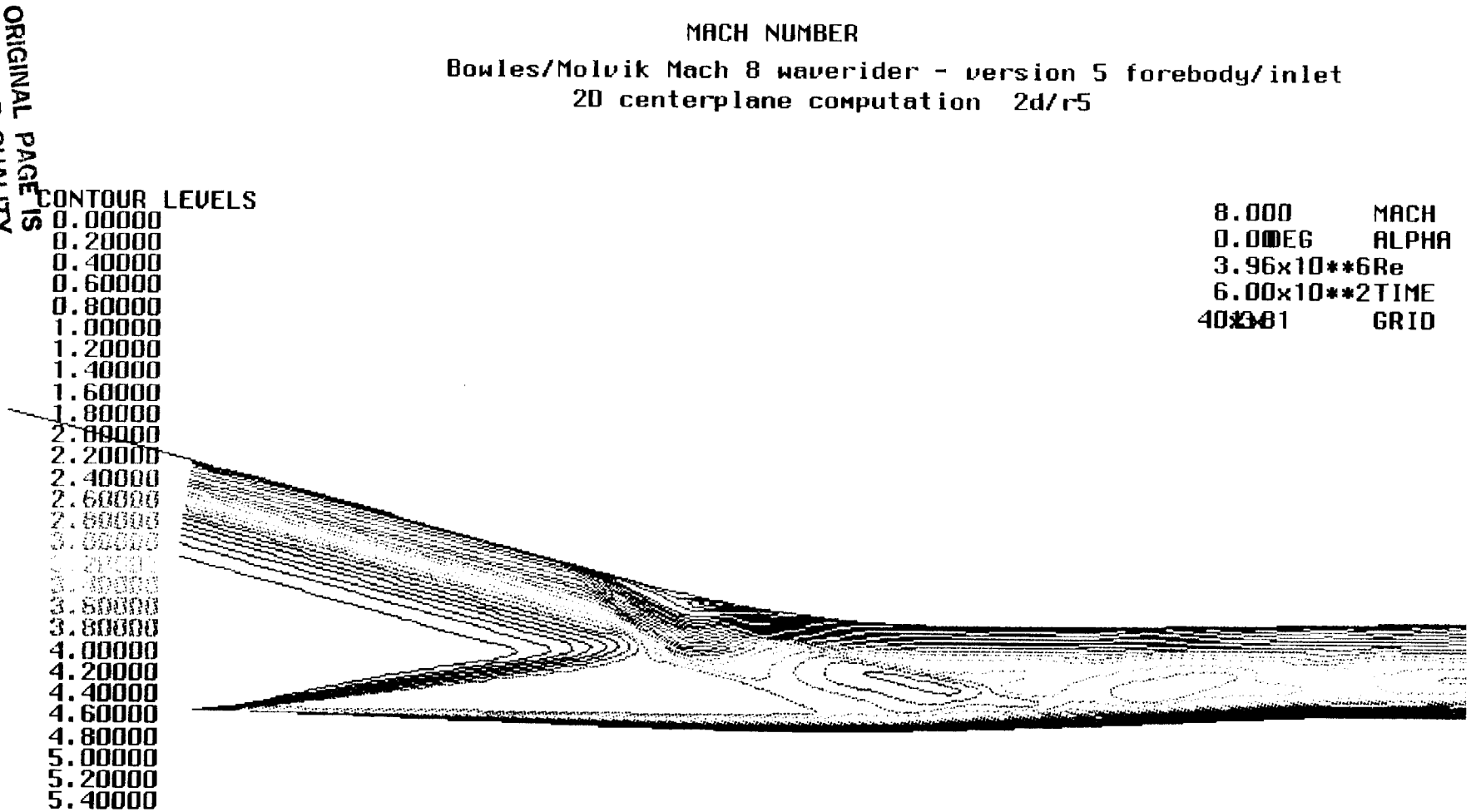

FIGURE 17 **OVERFLOW two-dimensional forebody/inlet solution of the redesigned (version 5) inlet at $M_\infty = 8.0$.**

a) **Mach number contours at the centerplane**

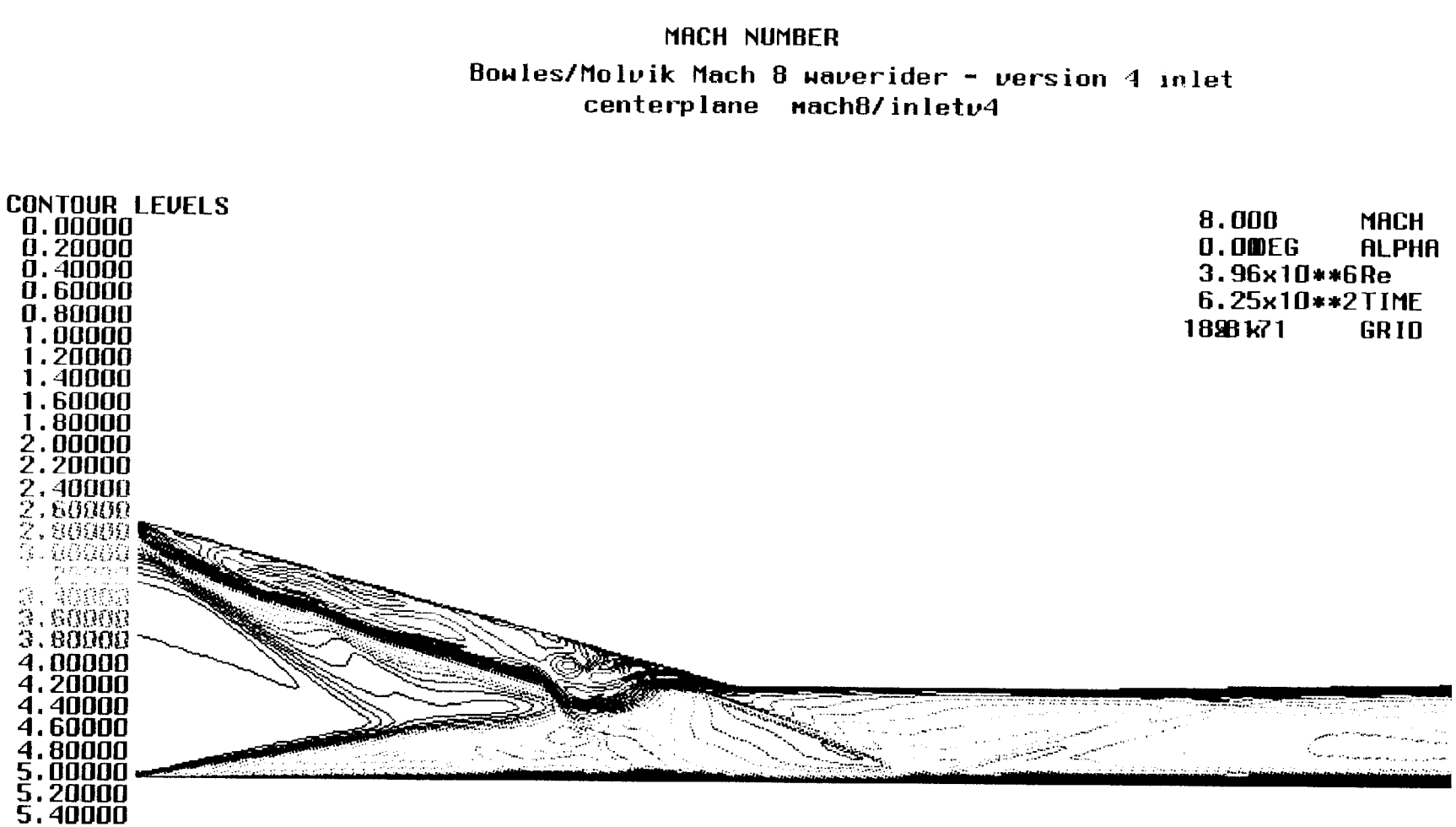

FIGURE 18 **OVERFLOW three-dimensional solution of baseline (version 4) inlet at $M_\infty = 8.0$.**

a) **Mach number contours at the inlet streamwise centerplane**

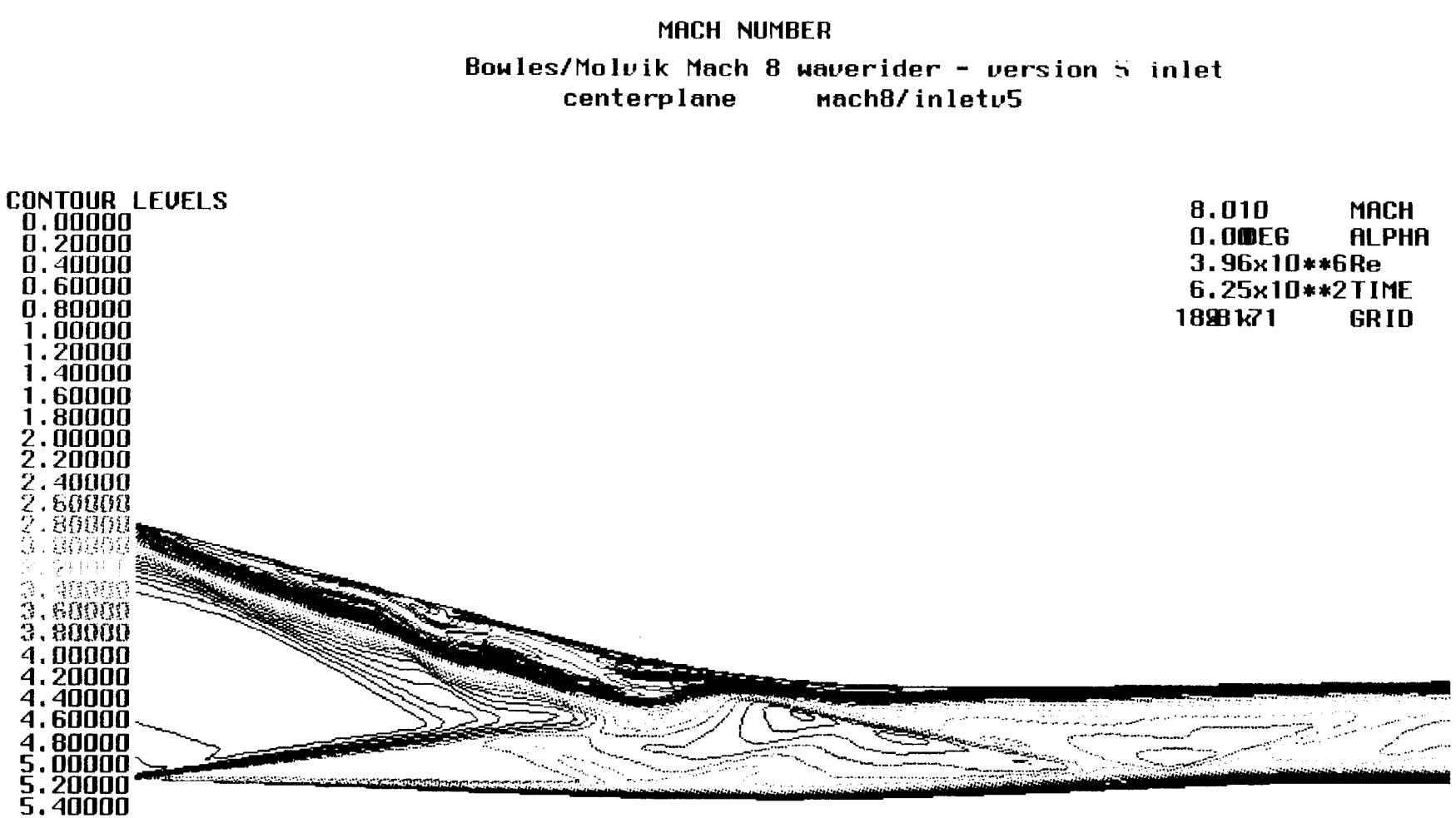

FIGURE 19 **OVERFLOW three-dimensional solution of redesigned (version 5) inlet at $M_\infty = 8.0$.**

a) **Mach number contours at the inlet streamwise centerplane**

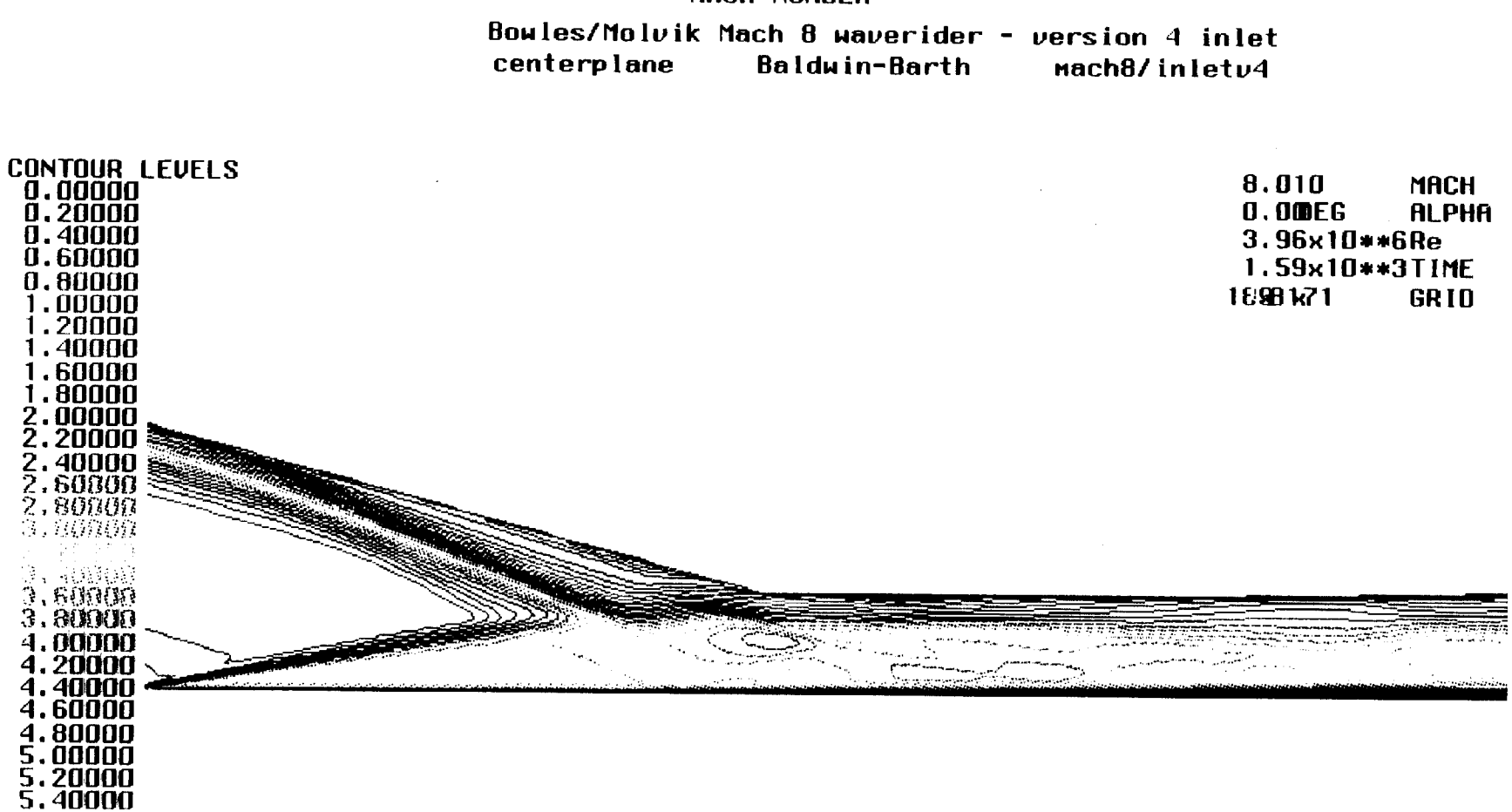

FIGURE 20 OVERFLOW three-dimensional solution of baseline (version 4) inlet at $M_\infty = 8.0$, Baldwin-Barth model.

a) Mach number contours at the inlet streamwise center plane

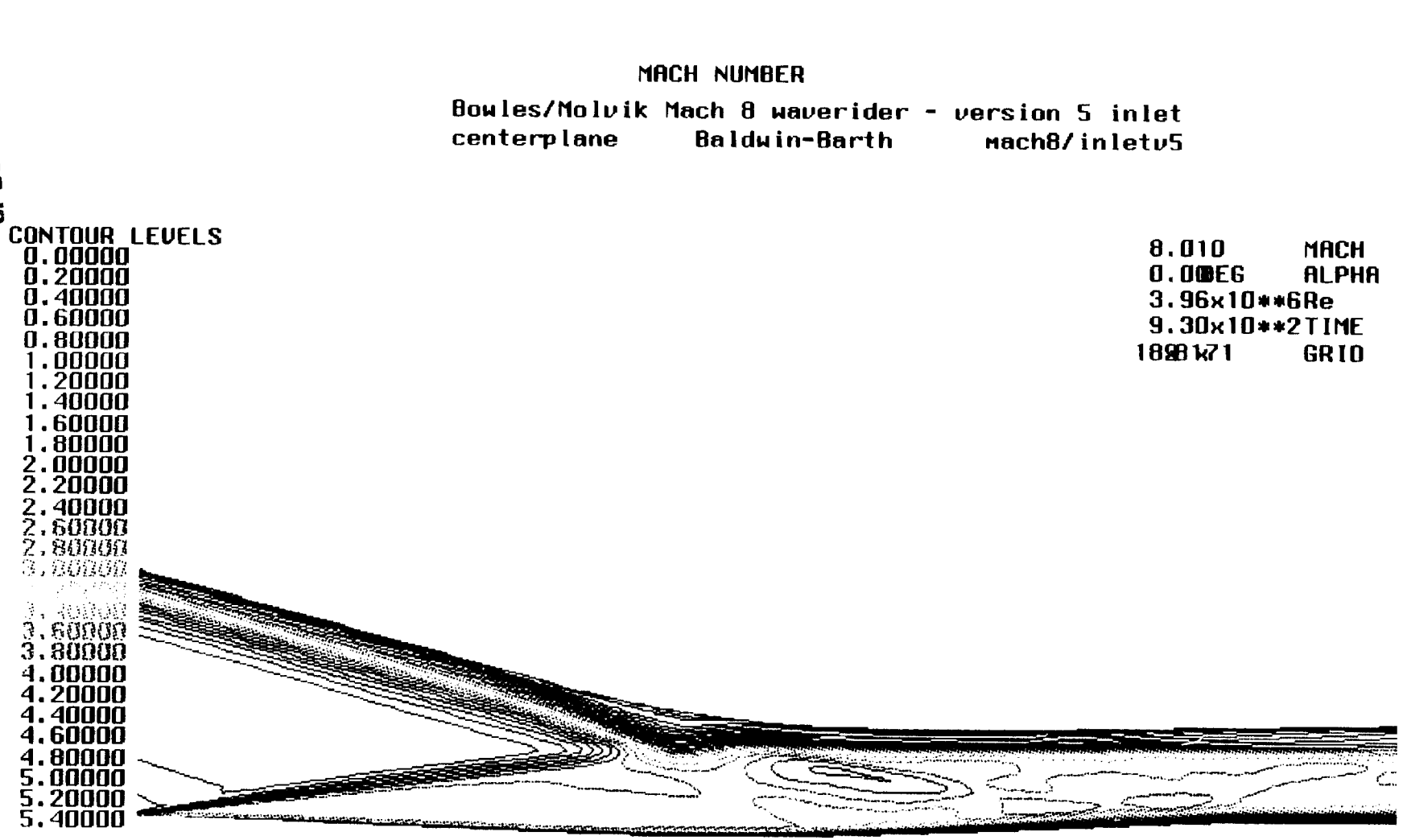

FIGURE 21 OVERFLOW three-dimensional solution of redesigned (version 5) inlet at $M_\infty = 8.0$, Baldwin-Barth model.

a) Mach number contours at the inlet streamwise center plane